Role of AP1 and Gadkin in the traffic of secretory endo-lysosomes

Karine Laulagnier[a,*], Nicole L. Schieber[b], Tanja Maritzen[c], Volker Haucke[c], Robert G. Parton[b], and Jean Gruenberg[a]

[a]Department of Biochemistry, University of Geneva, 1211-Geneva-4, Switzerland; [b]Institute for Molecular Bioscience and Center for Microscopy and Microanalysis, The University of Queensland, Brisbane 4072, Australia; [c]Laboratory of Membrane Biochemistry, Freie Universitaet Berlin, 14195 Berlin, Germany

ABSTRACT **Whereas lysosome-related organelles (LRO) of specialized cells display both exocytic and endocytic features, lysosomes in nonspecialized cells can also acquire the property to fuse with the plasma membrane upon an acute rise in cytosolic calcium. Here, we characterize this unconventional secretory pathway in fibroblast-like cells, by monitoring the appearance of Lamp1 on the plasma membrane and the release of lysosomal enzymes into the medium. After sequential ablation of endocytic compartments in living cells, we find that donor membranes primarily derive from a late compartment, but that an early compartment is also involved. Strikingly, this endo-secretory process is not affected by treatments that inhibit endosome dynamics (microtubule depolymerization, cholesterol accumulation, overexpression of Rab7 or its effector Rab-interacting lysosomal protein [RILP], overexpression of Rab5 mutants), but depends on Rab27a, a GTPase involved in LRO secretion, and is controlled by F-actin. Moreover, we find that this unconventional endo-secretory pathway requires the adaptor protein complexes AP1, Gadkin (which recruits AP1 by binding to the γ1 subunit), and AP2, but not AP3. We conclude that a specific fraction of the AP2-derived endocytic pathway is dedicated to secretory purposes under the control of AP1 and Gadkin.**

Monitoring Editor
Sandra Schmid
Scripps Research Institute

Received: Mar 8, 2011
Revised: Apr 12, 2011
Accepted: Apr 19, 2011

INTRODUCTION

After clathrin-dependent or -independent endocytosis, internalized solutes and membrane components, including receptors, reach early endosomes (Mayor and Pagano, 2007). From there, some molecules are recycled back to the plasma membrane, whereas others are transported to the *trans*-Golgi network (TGN) or to late endosomes and lysosomes. Along the latter pathway, molecules that need to be degraded, in particular down-regulated signaling receptors, are incorporated into nascent multivesicular endosomes, transported along microtubules toward late endosomes (Gruenberg, 2001), and eventually delivered to lysosomes for degradation (Luzio *et al.*, 2007). Other transport routes connect endosomes or lysosomes to the plasma membrane. Some specialized cells also contain lysosome-related organelles (LROs), including melanosomes in melanocytes, dense granules in platelets, and lytic granules in cytotoxic T lymphocytes, which exhibit lysosomal characteristics together with exocytic functions (Raposo *et al.*, 2002; Clark and Griffiths, 2003).

In nonspecialized fibroblast-like cells, a transient rise in intracellular Ca^{++} is believed to trigger the fusion of lysosomes with the plasma membrane (Rodriguez *et al.*, 1997; Andrews, 2000), in a process regulated by synaptotagmin VII (Czibener *et al.*, 2006) and dependent on the SNAREs (SNAP [Soluble NSF Attachment Protein] Receptor) VAMP7, syntaxin 4, and SNAP23 (Rao *et al.*, 2004). This lysosome-to-plasma membrane transport pathway is proposed to play a role in plasma membrane repair, entry of parasites, and tumor cell invasiveness (Rodriguez *et al.*, 1997; Reddy *et al.*, 2001; Andrews, 2002; Kroemer and Jaattela, 2005; Eder, 2009). In

This article was published online ahead of print in MBoC in Press (http://www.molbiolcell.org/cgi/doi/10.1091/mbc.E11-03-0193) on April 27, 2011.

*Present addresss: Laboratoire de Biologie Moléculaire de la Cellule, CNRS/ENS Lyon, 46 allée d'Italie, 69364 Lyon Cedex 07, France.

Address correspondence to: Jean Gruenberg (jean.gruenberg@unige.ch).

Abbreviations used: AP, adaptor protein complexes; BFA, brefeldin A; BSA, bovine serum albumin; CHC, clathrin heavy chain; DAB, diaminobenzidine; EGF, epidermal growth factor; EGTA, ethylene glycol tetraacetic acid; GFP, green fluorescent protein; HRP, horseradish peroxidase; KD, knockdown; LBPA, lysobisphosphatidic acid; LDH, lactate dehydrogenase; LRO, lysosome-related organelles; M6PR, mannose-6-phosphate receptor; NPC, Niemann–Pick C; PBS, phosphate-buffered saline; PFA, paraformaldehyde; RILP, Rab-interacting lysosomal protein; Tfn-R, transferrin receptor; TGN, *trans*-Golgi network; TIRF, total internal reflection fluorescence; WT, wild type.

addition, at least in some cell types, multivesicular endosomes—or some specialized subpopulation—may acquire the capacity to fuse with plasma membrane, and thereby release their intralumenal vesicles in the extracellular milieu as exosomes. On release, exosomes may modulate the immune response when produced by antigen-presenting cells (Raposo *et al.*, 1997; Denzer *et al.*, 2000; Stoorvogel *et al.*, 2002; Zeelenberg *et al.*, 2008), but may also mediate the secretion of PLP protein in oligodendrocytes (Trajkovic *et al.*, 2008) and miRNAs (Gibbings *et al.*, 2009; Lee *et al.*, 2009). It is not clear to what extent these pathways may involve different endo-lysosomal subpopulations and share common mechanisms.

Studies of genetic syndromes with LRO deficiencies (e.g., Hermansky–Pudlak and Griscelli syndromes) have shown that the β and δ subunits of the adaptor protein complex AP3 and the Rab27a GTPase are essential for the biogenesis and/or exocytosis of melanosomes, platelet-dense granules, and lytic granules (Novak *et al.*, 2002; Raposo *et al.*, 2007). In melanocytes, both AP1 and AP3 are necessary for cargo sorting to maturing melanosomes (Theos *et al.*, 2005; Raposo *et al.*, 2007; Groux-Degroote *et al.*, 2008; Delevoye *et al.*, 2009). Interestingly, whereas melanosome maturation from early endosomes may involve a separate pathway parallel to that mediating conventional lysosomes biogenesis (Raposo *et al.*, 2007), lytic granules represent the only identified lysosomal organelles of cytotoxic T-cells. In nonspecialized cells, AP1 and AP3 are also required for targeting lysosomal membrane proteins (e.g., Lamp1, Lamp2) and mannose-6-phosphate receptor (M6PR) to endosomes and/or lysosomes (Le Borgne *et al.*, 1998; Reusch *et al.*, 2002; Ihrke *et al.*, 2004). It has also been proposed that Lamps may be transported to lysosomes indirectly via the plasma membrane and AP2-mediated endocytosis (Lippincott-Schwartz and Fambrough, 1987; Janvier and Bonifacino, 2005). Hence, the precise composition of the machinery and the biogenesis of lysosomal secretory organelles may vary from one cell type to another (Clark and Griffiths, 2003).

In this article, we have followed Lamp1 appearance on the plasma membrane and lysosomal enzyme release into the medium on an acute rise in cytosolic calcium to characterize the membranes involved in this unconventional secretory process. Our data indicate that membranes primarily, but not exclusively, derived from a late compartment, gain the capacity to fuse with the plasma membrane, but fail to acquire characteristic endosomal properties. Our data suggest that sorting into this pathway involves AP1, the AP1 recruitment factor Gadkin, and an AP2-dependent step and that Rab27a regulates trafficking along this route. We conclude that fibroblast-like cells contain specialized endosomal compartments or subcompartments, akin to LROs, which can support fusion with the plasma membrane when triggered.

RESULTS

Calcium-induced exocytosis of hexosaminidase and Lamp1

We used the calcium ionophore, ionomycin, to induce a transient rise in cytosolic calcium concentration. To avoid possible toxic effects of the drug, we optimized the conditions of the treatment (see *Materials and Methods*) so that cell survival (unpublished data) was not affected. Cell integrity was measured by the release of the abundant cytosolic enzyme lactate dehydrogenase (LDH) into the culture medium (Figure 1A). Because LDH release occurred after prolonged incubation with ionomycin (Figure 1B), all studies were performed at earlier time points (≤10 min). After the ionomycin treatment, small but significant amounts of hexosaminidase, a lysosomal enzyme, were released into the extracellular medium, corresponding to ≈1% of the total cell-associated activity in A431 (Figure 1A) and BHK cells (Figure 1B). This release was abolished by ethylene glycol tetraacetic acid (EGTA) in the medium (Figure 1B). Consistently, we found that ionomycin induced the appearance of Lamp1 at the plasma membrane, a process that could be unambiguously observed by immunofluorescence in nonpermeabilized BHK (Figure 1C, left panels). An analysis by time-lapse total internal reflection fluorescence (TIRF) microscopy confirmed that ionomycin addition caused Lamp1 to diffuse in rapid flashes away from punctae close to the plasma membrane, presumably corresponding to the fusion of individual Lamp1-positive vesicles with the plasma membrane (Supplemental Movie 1). Cell permeabilization revealed that, much like with hexosaminidase (Figure 1A), the majority of Lamp1 remained intracellular with only a minor proportion being transferred to the plasma membrane (Figure 1C, right panels). To quantify Lamp1 transport to the plasma membrane, the cell surface was biotinylated after ionomycin treatment (Parton *et al.*, 1992; Gottardi *et al.*, 1995). Lamp1 rapidly appeared at the plasma membrane and reached a plateau within 5–10 min with a 10-fold increase over nonstimulated controls (Figure 1, D and E, quantification in F), corresponding to 2–3% of total cellular Lamp1 (Figure 1D). Much like hexosaminidase release (Figure 1B), the process was abolished by calcium chelation with EGTA (Figure 1, E and F). By contrast, actin was not biotinylated, confirming that cells remained intact during the experiment (Figure 1, D and E). We also observed that biotinylation of cell surface transferrin receptor (Tfn-R) was slightly increased, perhaps suggesting that a small fraction of Tfn-R follows the same calcium-dependent exocytic route as Lamp1 or that a calcium rise also triggers exocytosis from some early/recycling endosome subpopulation. In any case, our observations, which confirm previous studies (Rodriguez *et al.*, 1997; Andrews, 2000), support the notion that a calcium rise triggers the fusion of compartments containing hexosaminidase and Lamp1 with the plasma membrane.

Exocytosis of hexosaminidase and Lamp1 is insensitive to cholesterol overload

To better characterize the donor compartment involved in the delivery of hexosaminidase and Lamp1 to the plasma membrane, we made use of our observations that U18666A, a drug that mimics the cholesterol storage disorder Niemann–Pick C (NPC), causes a paralysis of late endocytic compartments, which become clustered in the perinuclear region of the cell (Liscum *et al.*, 1989**;** Ko *et al.*, 2001; Zhang *et al.*, 2001; Lebrand *et al.*, 2002). As a result, transport from late endosomes to other cellular destinations is inhibited, including recycling of CD63 to Weibel–Palade bodies in endothelial cells (Kobayashi *et al.*, 2000) and of M6PR to the TGN (Kobayashi *et al.*, 1999). Similarly, lysosome fusion at the ruffled border of osteoclasts is inhibited by U18666A-mediated cholesterol accumulation in late endocytic compartments (Zhao and Vaananen, 2006).

As expected, cholesterol was predominantly present in the plasma membrane of control cells and accumulated in perinuclear structures containing Lamp1 after drug treatment (Figure 2, A and D). Strikingly, however, U18666A had essentially no effect on hexosaminidase release (Figure 2B) and Lamp1 appearance at the plasma membrane measured by light microscopy (Figure 2A), or cell surface biotinylation (Figure 2C). Neither was the small increase in Tfn-R biotinylation observed after ionomycin treatment sensitive to U18666A treatment. Similarly, endocytosed antibodies against the late endocytic lipid lysobisphosphatidic acid (LBPA; Kobayashi *et al.*, 1998), which also cause cholesterol accumulation in late endocytic compartments and phenocopy NPC (Kobayashi *et al.*, 1999), failed to affect Lamp1 appearance at the plasma membrane in ionomycin-treated cells (Supplemental Figure S1A).

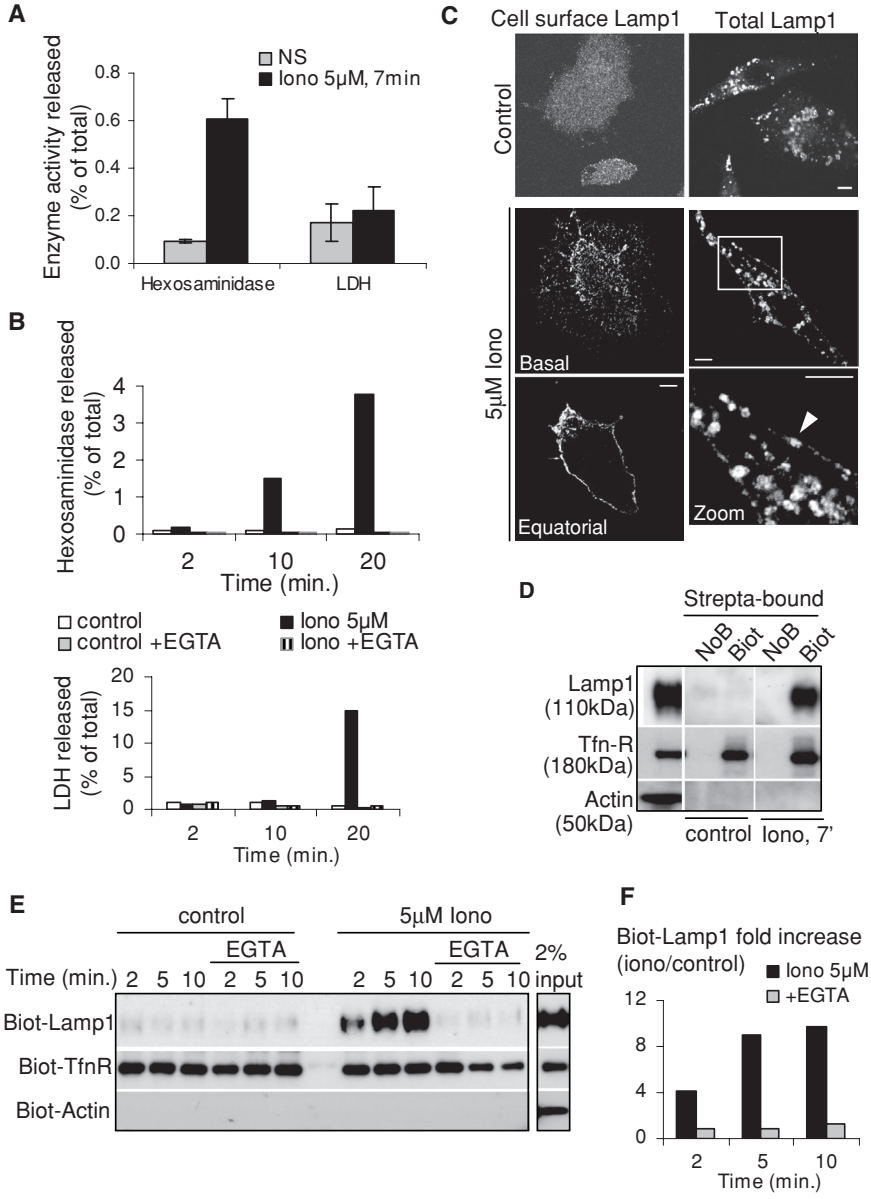

FIGURE 1: Ionomycin-induced release of hexosaminidase and transport of Lamp1 to the plasma membrane. (A and B) A431 cells (A) or BHK cells (B) were stimulated with 5 μM ionomycin (Iono) or not (NS) for the indicated time. Then hexosaminidase or LDH activity was measured in the medium and in total cell lysates. The enzyme activity released in the medium is expressed as a percentage of the total activity in lysates. (A) shows the mean ± SEM of five and four experiments for hexosaminidase and LDH, respectively, and (B) shows typical kinetics of ionomycin stimulation with or without 1 mM EGTA. No LDH release was observed before 10 min of ionomycin stimulation. (C) BHK cells were stimulated or not as in A and incubated on ice with anti-Lamp1 antibodies without permeabilization (left column, "cell surface Lamp1"), fixed with PFA and labeled with fluorescent secondary antibody. Pictures after Z-stacking show homogeneous Lamp1 distribution on the cell surface ("Basal") and a clear peripheral labeling at the equatorial Z-position ("Equatorial"). Alternatively, cells were fixed, permeabilized, and labeled with anti-Lamp1 antibodies to reveal total Lamp1 (right column). After stimulation, we observed little change in the distribution of intracellular Lamp1, but peripheral labeling was sometimes observed (arrowhead) as shown in the high magnification view of the boxed area. Bars = 5 mm. (D–F) After stimulation as in A and B, cell surface proteins of BHK (D) or A431 (E and F) were biotinylated ("Biot") on ice and lysed. In controls, the biotinylation agent was omitted (NoB). Lysates were incubated with streptavidin-coated beads, and bound biotinylated proteins ("strepta-bound") were eluted, separated by SDS gel, and analyzed by Western blotting using the indicated antibodies. (D) 3% and (E) 2% from nonstimulated lysates were separated in parallel. (F) The experiment in E was quantified, and the ratio of stimulated versus nonstimulated biotinylated-Lamp1 signals is shown. The results were normalized to biot-TfnR signal and are expressed as "fold increase."

When analyzed by time-lapse video microscopy, Lamp1-containing membranes exhibited high motility across the whole cell cytoplasm (Supplemental Movie 2), whereas in U18666A-treated cells the bulk of Lamp1 was immobile (Supplemental Movie 3) and clustered in perinuclear cholesterol-containing membranes (Figure 2D). Interestingly, despite U18666A treatment, a few Lamp1-positive vesicles remained motile (Supplemental Movie 3) at the cell periphery and did not accumulate cholesterol (Figure 2, D and E). Indeed, peripheral motile endosomes containing Lamp1 were observed by TIRF time-lapse microscopy in U18666A-treated cells (see Figure 5C later in the paper and Supplemental Movie 4) as in untreated controls (see Figure 5A later in the paper and Supplemental Movie 5). Similarly, motile vesicles labeled with LysoTracker have been observed in U18666A-treated cells (Rocha *et al.*, 2009). This small subpopulation of cholesterol-free and motile Lamp1 compartments that we observed could represent the vesicles that are competent for fusion with the plasma membrane.

Exocytosis of hexosaminidase and Lamp1 depends on Rab27a and actin but not on known endo-lysosomal regulators

Our observations with U18666A suggest that the exocytosis of late endocytic subcompartments may not involve long-distance motion on microtubules to reach the cell periphery and the plasma membrane. Accordingly, depolymerization of the microtubules with nocodazole (Supplemental Figure S1B) or their stabilization with paclitaxel (unpublished data) had no effect on hexosaminidase release (Supplemental Figure S1C), Lamp1 appearance at the plasma membrane measured by immunofluorescence (Supplemental Figure S1B), or cell surface biotinylation (Supplemental Figure S1D), confirming previous observations (Reddy *et al.*, 2001).

In general, the dynamics of late endocytic membranes including maturation (Zerial and McBride, 2001), docking/fusion, and motility are controlled by the small GTPase Rab7 (Bucci *et al.*, 2000; Lebrand *et al.*, 2002), in part via the Rab7 effector RILP (Rab-interacting lysosomal protein), which regulates interactions with microtubules (Jordens *et al.*, 2001; Johansson *et al.*, 2007). Consistently, overexpression of Rab7-green fluorescent protein (GFP) or RILP-GFP clustered late endocytic compartments containing Lamp1 in the perinuclear region (Figure 3A), presumably at the minus ends of microtubules (Lebrand *et al.*, 2002; Johansson *et al.*, 2007). Ionomycin-induced Lamp1 appearance at the plasma membrane remained unaffected, however (Figure 3B). Similarly, overexpression of the dominant-negative Rab7 mutant N125I had no effect on Lamp1 transport to the plasma membrane (Figure 3B). Neither did the dominant-negative deletion

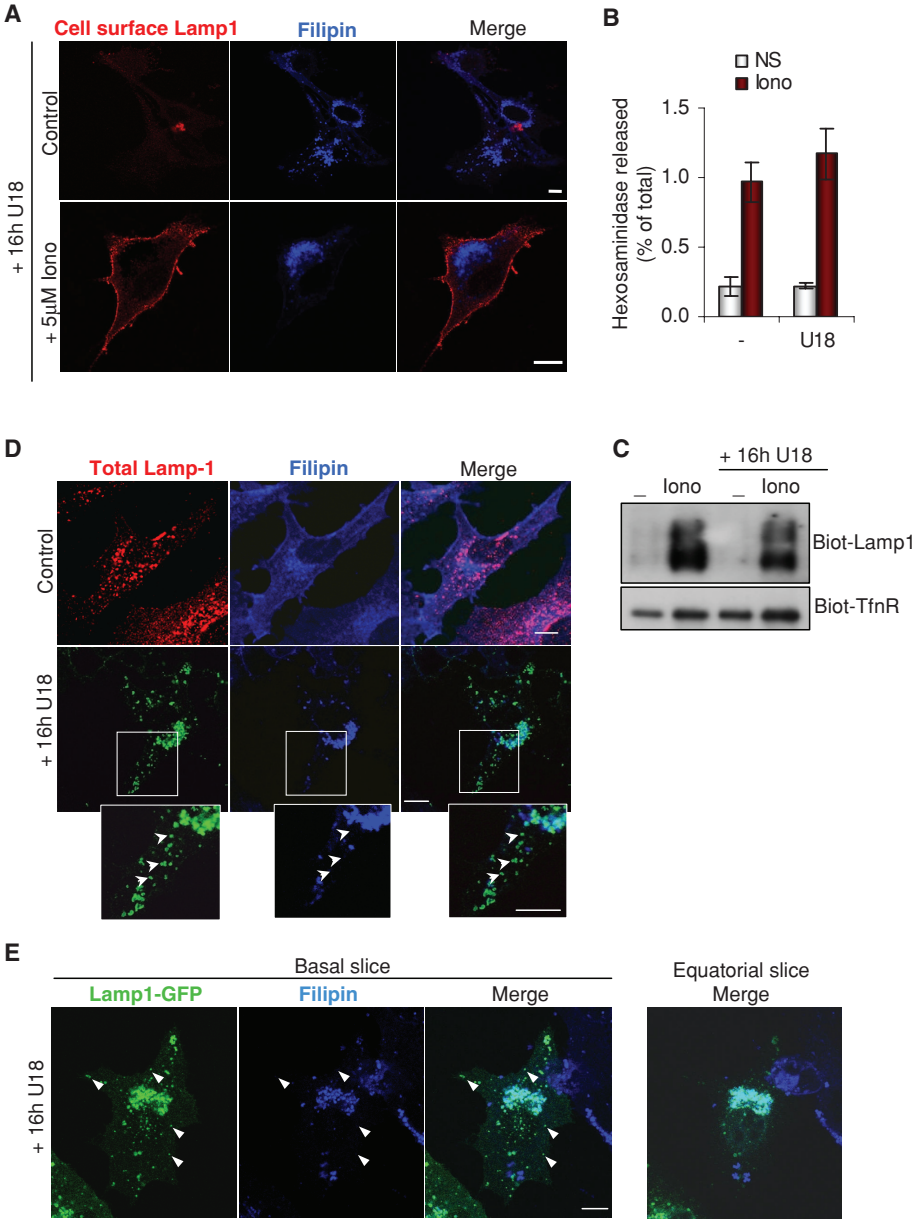

FIGURE 2: Cholesterol accumulation does not impair the release of hexosaminidase and the transport of Lamp1 to the plasma membrane. (A) BHK cells treated with 3 mg/ml U18666A for 16 h ("16h U18") were stimulated or not with ionomycin as in Figure 1A, labeled with anti-Lamp1 antibodies before fixation, and stained with filipin to reveal cholesterol. Bars = 10 µm. (B and C) Cells were treated with U18666A before stimulation with ionomycin as in (A), and hexosaminidase release (B) was measured as in Figure 1A. Mean ± SEM of three experiments is shown. In parallel, cell surface biotinylation (C) was analyzed as in Figure 1D. (D) Control cells or cells treated with U18666A were fixed, permeabilized, and double-labeled with filipin and anti-Lamp1 antibodies. High magnification view of the boxed area shows Lamp1-positive structures in the cell periphery that are not labeled by filipin (arrowheads). (E) BHK cells were transfected with Lamp1-GFP, treated with U18666A, fixed, and labeled with filipin. Basal slice of Z-stacking is shown in comparison to an equatorial Z slice (right panel, only merge shown). Arrowheads point at peripheral Lamp1-GFP structures devoid of cholesterol.

mutant of RILP C33 (Figure 3B), although these mutants affected the distribution of late endosomes and lysosomes (unpublished data; Cantalupo *et al.*, 2001). Similarly, hexosaminidase release was not affected by overexpression of wild type (WT) or mutant Rab7 or RILP (Figure 3C). Interestingly, exosome release seems to be similarly independent of Rab7 (Ostrowski *et al.*, 2010). Consistent with these findings, we found that overexpression of the small GTPase Rab5, which controls endocytic traffic upstream of Rab7 (Zerial and McBride, 2001), or the constitutively active or dominant-negative Rab5 mutants did not affect Lamp1 appearance at the plasma membrane after ionomycin treatment (Figure 3D).

Because we did not observe a role for Rab7, we wondered whether another GTPase regulated this secretory process. Rab27a, which is known to control LRO biogenesis and trafficking (Fukuda, 2005) as well as exosome release (Ostrowski *et al.*, 2010), was a strong candidate. In accordance with this hypothesis, Rab27a depletion with siRNAs, albeit only partial (≈80% when compared with the mock-treated control), significantly reduced both hexosaminidase release (Figure 4A) and Lamp1 appearance at the plasma membrane (Figure 4B). This finding suggests that Rab27a regulates this unconventional secretory process in fibroblast-like cells, as it does for the secretion of LROs in specialized cells. Consistent with this notion, an analysis using the GENEVESTIGATOR Web site (https://www.genevestigator.com/gv/index.jsp), which combines thousands of microarray experiments, shows that the Rab27a transcript is present in all tissues and cell types.

Although microtubules appeared to play no role in this unconventional secretory process (Supplemental Figure S1, B–D), we found that depolymerization of the actin cytoskeleton with latrunculin B (Figure 4C) increased hexosaminidase release (Figure 4D) and the appearance of Lamp1 on the cell surface (Figure 4E) after ionomycin treatment, as expected from previous findings (Rodriguez *et al.*, 1997; Jaiswal *et al.*, 2002). It should be noted that Tfn-R appearance at the plasma membrane was not affected by Rab27 knockdown (KD). Presumably, depolymerization of the cortical actin cytoskeleton facilitates access to the plasma membrane, in agreement with the role of F-actin in the capture of LROs (Desnos *et al.*, 2003; Barral and Seabra, 2004). These findings agree well with the notion that Rab27a regulates interactions with the actin cytoskeleton in close proximity to the plasma membrane (Barral and Seabra, 2004). Consistent with this view, motile vesicles containing both Lamp1 and Rab27A were observed by using TIRF microscopy in close vicinity of the plasma membrane. (Figure 5A shows snapshots of Supplementary Movie 5). After ionomycin addition, Rab27a became more diffuse at the same time as Lamp1 (Figure 5B shows snapshots of Supplementary Movie 1), presumably reflecting the occurrence of vesicle fusion with the plasma membrane (Jaiswal *et al.*, 2002). Altogether, these results indicate that a small subpopulation of Lamp1-, Rab27a-, and hexosaminidase-containing membranes acquires the capacity to dock onto and fuse with the plasma

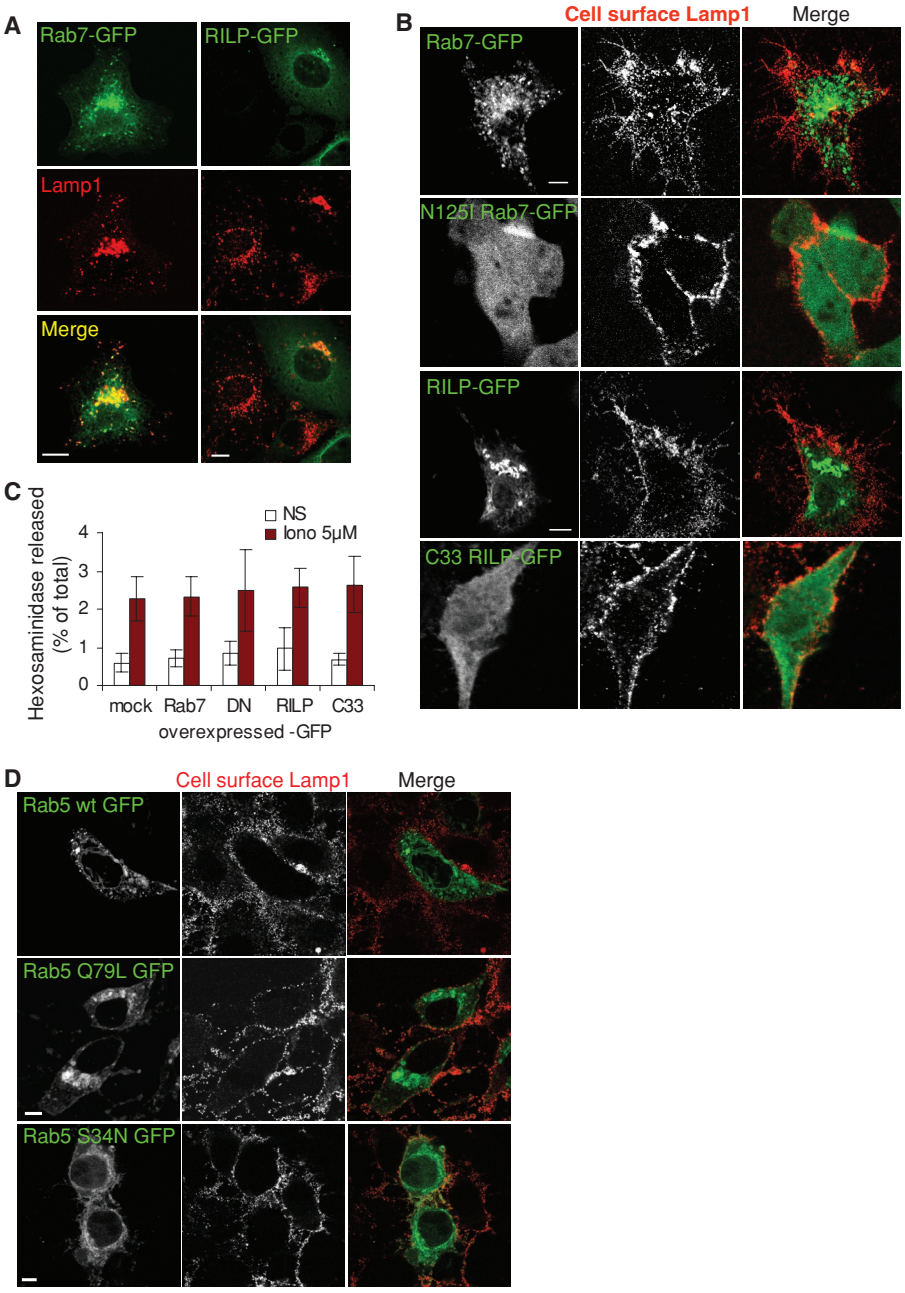

FIGURE 3: Endo-lysosomal exocytosis is not under the control of Rab7, RILP, or Rab5. (A) BHK cells overexpressing WT Rab7-GFP or WT RILP-GFP were fixed, permeabilized, and labeled with anti-Lamp1 antibody. (B) Cells overexpressing the indicated constructs were stimulated as in Figure 1A, and then cell surface Lamp1 was revealed as in Figure 1C. (C) After stimulation, hexosaminidase release was measured in cells overexpressing the indicated constructs as in Figure 1A (mock: mock-treated; DN, dominant-negative mutant Rab7-N125I; C33, deletion mutant RILP-C33). Means ± SEM of three experiments are shown. (D) A431 cells overexpressing GFP-tagged WT, constitutively active Q79L mutant or dominant-negative S34N mutant Rab5 were treated as in (B). Bars = 10 mm.

membrane upon calcium rise, in a process that is independent of microtubules, cholesterol, and the late endocytic regulator Rab7, but regulated by the actin cytoskeleton and the small GTPase Rab27a.

Inhibition of biosynthetic membrane transport with brefeldin A

The observations just mentioned indicate that proteins of the late endocytic pathway were exocytosed upon calcium rise in a process that involved Rab27a and actin but did not require known regulators of late endocytic traffic. These surprising observations, combined with the fact that only low amounts of hexosaminidase and Lamp1 reached the plasma membrane after ionomycin treatment, prompted us to investigate whether the donor compartment in this unconventional secretory process was of biosynthetic rather than endocytic origin.

Cells were thus treated with brefeldin A (BFA), a drug that rapidly arrests biosynthetic membrane transport (Klausner *et al.*, 1992). Although the drug was active, as assessed by the dispersal of the TGN marker TGN38 (Figure 5D), it had no effect on hexosaminidase release (Figure 5E) or Lamp1 biotinylation at the plasma membrane (Figure 5F) even 1 h after addition. To better characterize the effects of BFA, we made use of the fact that cathepsin D is synthesized as a large 52 kDa precursor (proform), which is then processed to an intermediate 48 kDa form and eventually to the mature and active 29 kDa enzyme in lysosomes (Gieselmann *et al.*, 1983; Zaidi *et al.*, 2008). Consistent with the fact that low amounts of the precursor forms of cathepsin D are secreted constitutively at least in some cell types (Ludwig *et al.*, 1991, 1994), low levels of immature cathepsin D were detected in the supernatant of nonstimulated cells (Figure 5G), and this process was inhibited by BFA (Figure 5G). In agreement with our hexosaminidase and Lamp1 data (Figure 1), ionomycin stimulated mature cathepsin D release into the extracellular medium and also slightly increased the secretion of immature forms (Figure 5G). Strikingly, BFA had essentially no effect on the release of the mature enzyme into the extracellular medium, although secretion of the newly synthesized precursor forms remained BFA-sensitive, as expected (Figure 5G). These experiments thus show that the calcium-dependent release of hexosaminidase, Lamp1, and mature cathepsin D does not involve the biosynthetic pathway directly, and most likely occurs from endocytic membranes.

Ablation of endocytic compartments by HRP-mediated cross-linking

Because low amounts of hexosaminidase and Lamp1 could also be present earlier in the endocytic pathway, we wanted to determine precisely which endocytic compartment is involved in this unconventional secretory process. To this end, we used an horseradish peroxidase (HRP)-mediated chemical cross-linking protocol to selectively ablate endosome or lysosome populations in living A431 cells (Stoorvogel, 1998). First, HRP-conjugated Tfn was endocytosed for 15 min at 37°C, and then cells were incubated with diaminobenzidine (DAB) and low H_2O_2 concentrations (Stoorvogel, 1998; Brachet *et al.*,

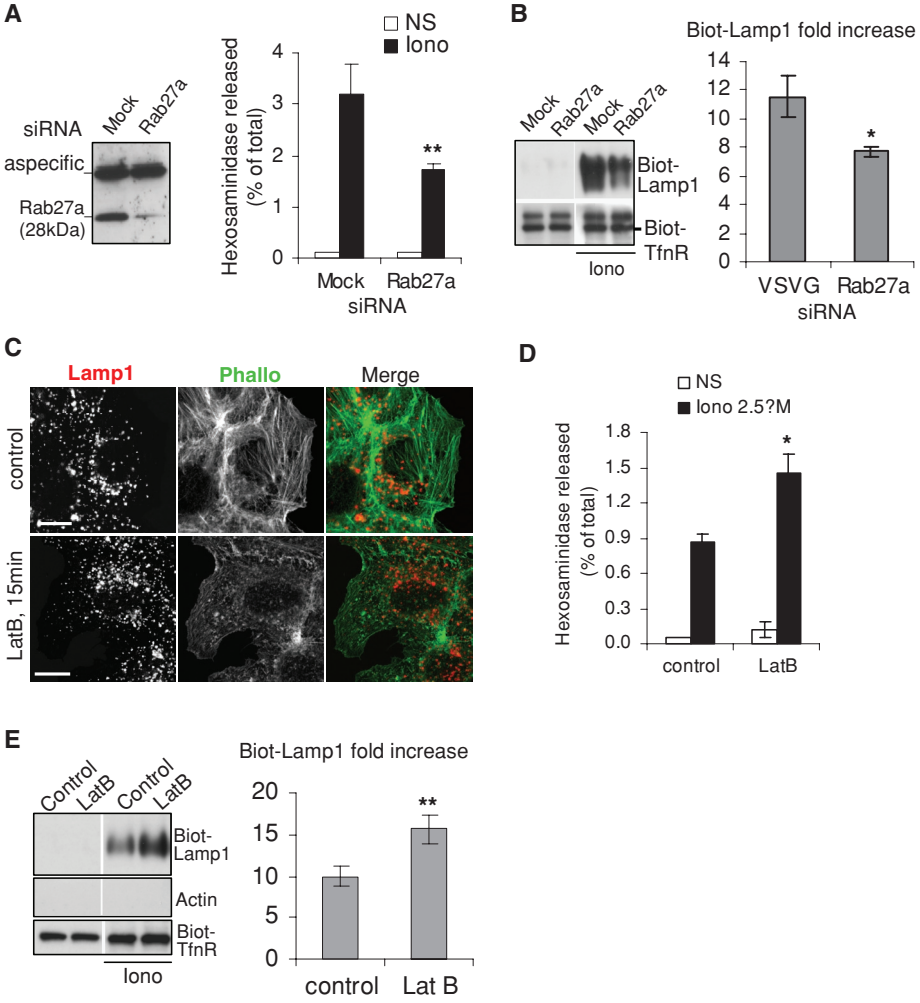

FIGURE 4: Role of Rab27a and F-actin in the release of hexosaminidase and the transport of Lamp1 to the plasma membrane. (A and B) A431 cells were transfected with siRNA against human Rab27a and analyzed by Western blot (≈85% KD efficiency). The top band in panel A shows a cross-reaction of the antibody. Hexosaminidase release (A) and Lamp1 appearance on the plasma membrane after cell-surface biotinylation (B) were measured as in Figure 1, A, E, and F, respectively. A and B show the means ± SEM of four experiments. *$p < 0.04$, **$p < 0.025$. (C) A431 cells were treated for 15 min with 1 nM Latrunculin B before stimulation with 2.5 µM ionomycin. Cells were fixed in PFA, permeabilized, and labeled with Alexafluor 488 Phalloïdin and anti-Lamp1 antibody. Bar = 10 µm. (D and E) Cells were treated as in (C), and then the release of hexosaminidase (D) and Lamp1 appearance on the plasma membrane after cell surface biotinylation (E) were measured as in Figure 1, A, E, and F, respectively. (D and E) *$p < 0.04$; **$p < 0.025$.

1999), before stimulation with ionomycin. When analyzed by electron microscopy, electron-dense tubules and vesicles with the characteristic morphology of early and recycling endosomes were observed in cells treated with DAB, but not when DAB was omitted (Supplemental Figure S1E). This observation demonstrates that cross-linking by the polymeric oxidation product of DAB had occurred in the lumen of endosomes containing Tfn-HRP. The release of mature cathepsin D (Figure 6A) and hexosaminidase (Figure 6B), however, was not affected by the treatment. Next cells were incubated with 0.5 g/l HRP for 15 min at 37°C (pulse) to internalize HRP into early endosomes by fluid-phase endocytosis (Gruenberg *et al.*, 1989). Cross-linking caused by DAB polymerization, however, did not affect the release of hexosaminidase after ionomycin treatment (Figure 6B). Hexosaminidase release remained unaffected when the HRP pulse was followed by a 15-min chase at 37°C, but significantly decreased at later time points, ultimately reaching a minimal value, corresponding to approximately half the control after a 90-min chase (Figure 6B). Hexosaminidase release could be further decreased to approximately one-third of the control, when 10× higher HRP concentrations were used in the medium during the pulse. We thus conclude that hexosaminidase is primarily released from a compartment that becomes accessible to endocytosed HRP only after a long incubation time.

Electron microscopy analysis of the endocytic compartment containing HRP

To visualize the compartment that had been cross-linked by HRP, we carried out an analysis by using electron microscopy after HRP endocytosis under the same conditions as used in the ablation experiments (15-min pulse followed by a 90-min chase). This analysis revealed the presence of profiles labeled with HRP in the close vicinity of the plasma membrane without (Figure 6C) or with ionomycin stimulation (unpublished data). These profiles exhibited the characteristic tubulovesicular and multivesicular ultrastructure of late endosomal elements. To further characterize this compartment, cells transfected with Rab27a-GFP were incubated with HRP for 15 min followed by a 90-min chase without HRP as above, and processed for cryosectioning and immunogold labeling using antibodies against HRP, GFP, and Lamp1. Characteristic multivesicular endosomes containing HRP and Rab27a could be observed close to the plasma membrane, as well as multivesicular profiles containing Lamp1 and Rab27a without (Figure 6, D and E) or with (unpublished data) stimulation. These endosomes presumably correspond to the peripheral vesicles containing Lamp1 and Rab27a observed by TIRF microscopy (Figure 5A), and to the unconventional secretory compartment cross-linked by HRP in our ablation experiments (Figure 6).

HRP-mediated cross-linking inhibits cathepsin D release

To further characterize this compartment, we monitored the release of the immature and mature forms of cathepsin D in cells treated or not with HRP followed by DAB cross-linking. Interestingly, the secretion of cathepsin D proform, but not mature cathepsin D, was reduced after cross-linking of early endosomes with low or high concentrations of HRP pulsed for 15 min (Figure 6F). In agreement with our findings that proform secretion is BFA-sensitive (Figure 5), this result further supports the notion that the precursor forms of cathepsin D transit via early endosomes (Ludwig *et al.*, 1991). Similarly, we found that the secretion of cathepsin D proform was reduced by cross-linking early-recycling endosomes after Tfn-HRP endocytosis (Figure 6A). These observations indicate that some early endosomal elements may acquire the capacity to fuse with the plasma membrane, consistent with our observations that Tfn-R biotinylation

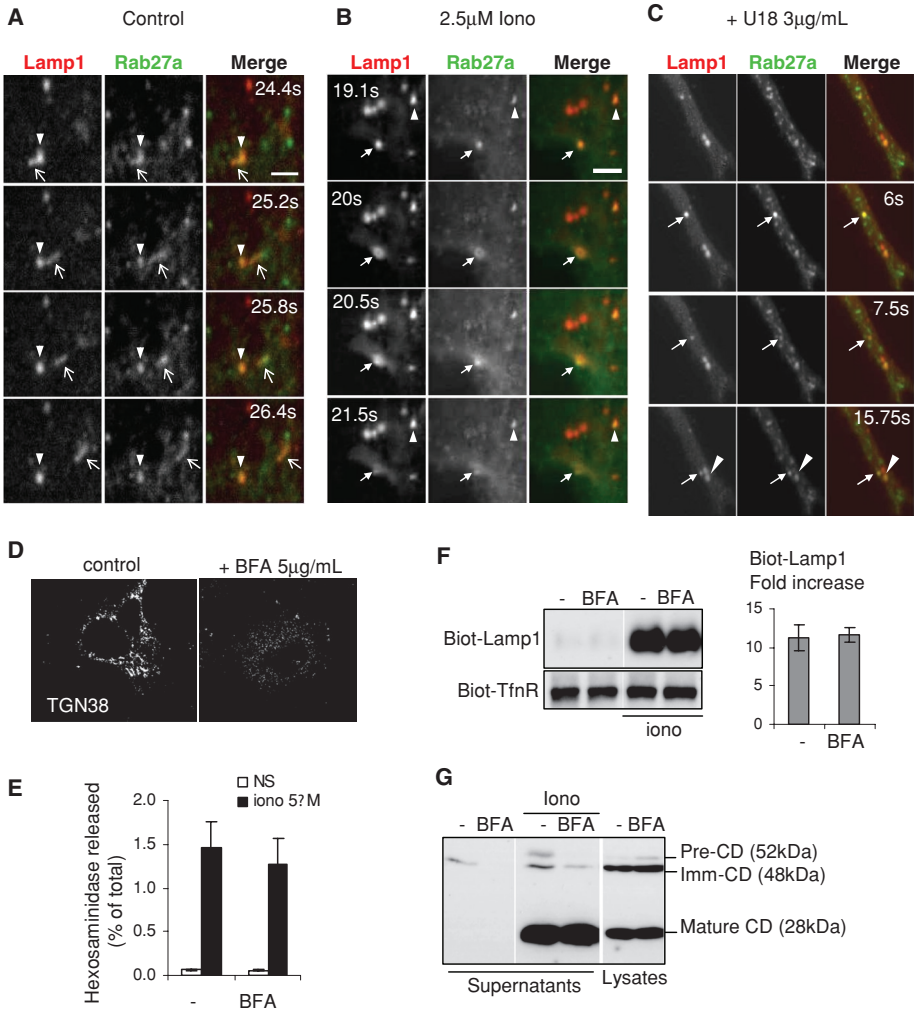

FIGURE 5: Regulation of endo-lysosomal exocytosis is controlled by Rab27a and is BFA-insensitive. (A and B) Living A431 cells overexpressing Rab27a-GFP (green) and Lamp1-cherry (red) were imaged by time-lapse TIRF microscopy at room temperature for 5 min without (A, control, see Supplemental Movie 5) or with 2.5 mM ionomycin (B, 2.5 µM Iono; see Supplemental Movie 1). Snapshots are shown for the indicated time points. Arrows point at a motile vesicle containing Rab27a and Lamp1, and an arrowhead points at an immobile reference in each frame. Bar = 2.5 µm. (C) As in (A), except that cells were pretreated with U18666A as in Figure 2A. Snapshots of Supplemental Movie 4 are shown for the indicated time points. Bar = 5 µm. (D--G) A431 cells were treated or not with 5 µg/ml BFA for 1 h before stimulation. (D) Cells were fixed, permeabilized, and labeled with anti-TGN38 antibody to monitor BFA effect. After BFA treatment, hexosaminidase release (E) was measured as in Figure 1A (means ± SEM of three experiments) or (F) cell surface proteins were biotinylated and analyzed as in Figure 1D. Panel F shows a representative blot and the quantification of three experiments (means ± SEM). (G) After stimulation, total proteins from cell supernatants were precipitated with TCA and blotted against cathepsin D (CD). Three percent of nonstimulated cell lysate was analyzed for comparison. The three cathepsin D isoforms are indicated on the blot.

at the cell surface is slightly increased after ionomycin treatment. In the presence of ionomycin, proform secretion remained sensitive to DAB-mediated cross-linking after chasing HRP for short (15–30 min), but not long (90 min) time periods (Figure 6F), presumably because some HRP remained in early endosomes after short times but was eventually chased from early endosomes at longer time points.

In marked contrast, however, secretion of mature cathepsin D was not affected by cross-linking with HRP pulses or short, 15-min chases, but was significantly reduced after a 30-min chase, particularly at high HRP concentrations, and essentially abolished after a 90-min chase (Figure 6F). Cell viability remained unaffected by the treatment after long chase time periods (unpublished data). Our data demonstrate that mature cathepsin D and active hexosaminidase are secreted when cytosolic calcium is acutely raised by ionomycin, and that the process is inhibited when late endocytic compartments are ablated by HRP-DAB cross-linking. Altogether, these data support the notion that secretion occurs primarily from a late endosome or lysosome subpopulation carrying the Rab27a GTPase in close vicinity of the plasma membrane.

Clathrin adaptors in lysosomal exocytosis

Adaptor complexes, in addition to their functions in transport between secretory and endocytic organelles, are also involved in LRO biogenesis in specialized cell types. We thus investigated whether adaptors play a role in the endo-lysosomal exocytic pathway(s) we have been studying. To this end, the µ subunit of AP1, AP2, or AP3 was depleted with siRNAs to ≈80% of the amounts present in the corresponding mock-treated control (Figure 7A).

The knockdown of each µ subunit did not affect total cellular levels of Lamp1 by Western blot (Figure 7B), nor did it cause significant changes in Lamp1 distribution by immunofluorescence (Figure 7C), consistent with the view that Lamp1 transport may occur via multiple routes (Reusch *et al.*, 2002; Bonifacino and Traub, 2003; Janvier and Bonifacino, 2005; Chapuy *et al.*, 2008). When analyzed further by confocal microscopy, the knockdown of µ1 or µ3 did not alter the steady-state distribution of Lamp1 at the plasma membrane of nonstimulated cells (Figure 7D). By contrast, after µ2 knockdown, Lamp1 accumulated at the plasma membrane already in nonstimulated cells (Figure 7D), consistent with the role of AP2-mediated endocytosis in Lamp1 cycling (Janvier and Bonifacino, 2005). Treatment with ionomycin did not further increase Lamp1 at the plasma membrane after µ2 knockdown, when compared with mock-treated controls (Figure 7D). By contrast, the knockdown of µ1 reduced the appearance of Lamp1 at the cell surface induced by ionomycin (Figure 7D), whereas µ3 knockdown did not seem to affect the process significantly.

To quantify these effects, we used our cell surface biotinylation protocol. As expected from the immunofluorescence data, Lamp1 accumulated at the surface of nonstimulated cells after µ2 knockdown—as did the Tfn-R, the cycling of which is also regulated by AP2-mediated endocytosis—and this accumulation was no longer sensitive to ionomycin treatment (Figure 7, E and F). Because biotinylated-Lamp1 did not further increase at the plasma membrane after ionomycin treatment, the amount of Lamp1 measured in ionomycin-treated cells divided by the amount in untreated cells (fold

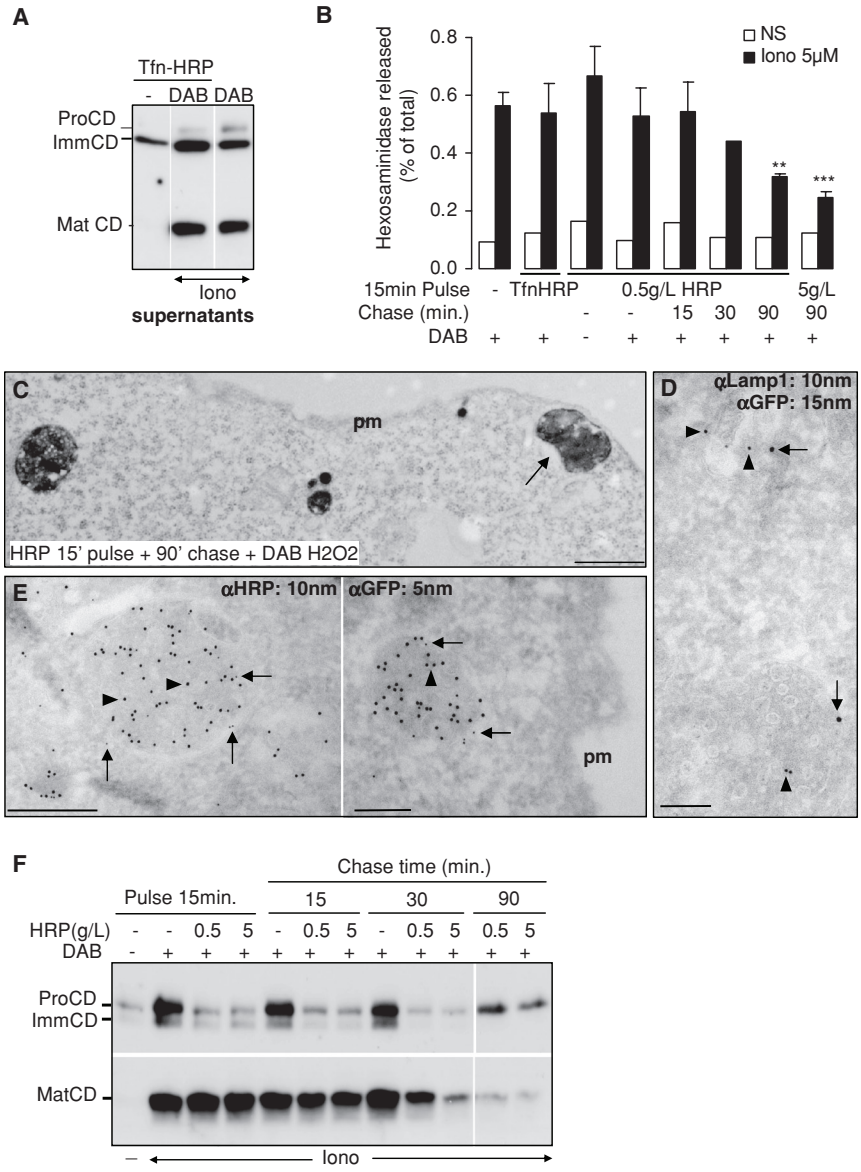

FIGURE 6: Identification of the endocytic organelles competent for secretion. (A) A431 cells were incubated with Tfn-HRP for 15 min at 37°C. Cells were treated without or with DAB–H_2O_2 as indicated to inactivate the compartment by cross-linking, and then stimulated or not with 5 μM ionomycin. Soluble proteins in the medium were precipitated with TCA and analyzed by Western blotting. We used antibodies that recognize the three main forms of cathepsin D (preCD, immature CD, mature CD) indicated on the figure. Note that this antibody recognized the precursor form with variable affinity. (B) A431 cells were incubated with Tfn-HRP or HRP (0.5 or 5 g/l as indicated) for 15 min at 37°C. Then endosomes containing HRP were cross-linked (DAB) as in A, or HRP was chased in HRP-free medium for the indicated time before cross-linking. After stimulation, hexosaminidase release was measured as in Figure 1A. The graph shows the means ± SEM of three Tfn-HRP experiments and four HRP experiments, except after a 30-min chase (two experiments). $^{**}p < 0.025$, $^{***}p < 0.0025$. Student's *t* test was done in comparison to the control condition with DAB only. (C) HRP (10 g/l) was endocytosed into BHK cells for 15 min at 37°C and then chased for 90 min, as in A. Samples were treated with DAB–H_2O_2 and processed for electron microscopy. Bar = 0.5 μm. (D–E) BHK cells overexpressing Rab27-GFP were incubated with HRP as in (B), and were processed for cryosectioning and immunogold labeling using antibodies (D) against GFP (arrows) and Lamp1 (arrowheads) or (E) against HRP (arrowheads) and GFP (arrows). Bar = 0.2 μm. (F) Cells were incubated with HRP and treated as in A. After stimulation, soluble proteins in the medium were precipitated with TCA, and were analyzed by Western blotting. We used antibodies that recognize cathepsin D mature form (Mat CD, bottom panels) or both pro- and immature forms (Pro- and Imm-CD, top panels). Blots allowed observation of the the main forms of cathepsin D (preCD, immature CD, mature CD) indicated on the figure. Note that the latter antibodies recognized the precursor form with variable affinity.

increase) was essentially equal to 1 after μ2 knockdown (Figure 7F). As expected (Figure 7D), Lamp1 was not detected at the plasma membrane without stimulation in μ1- or μ3-depleted cells. After μ3 knockdown, the addition of ionomycin caused a significant increase of Lamp1 at the plasma membrane (Figure 7, E and F; ≈12-fold increase), albeit to a somewhat lesser extent than in mock-treated controls (Figure 7F; ≈15-fold increase). This difference is presumably too small to be revealed by light microscopy (see Figure 7D). By contrast, μ1 knockdown reduced the appearance of Lamp1 at the plasma membrane induced by ionomycin significantly (Figure 7E), to approximately half of the control (Figure 7F), despite the fact that knockdown was not complete (Figure 7A).

Much like Lamp1 (Figure 7B), the total cellular levels of mature cathepsin D (Figure 7H, right panel) or active hexosaminidase (unpublished data) were not affected to any significant extent 72 h after knockdown of any of the μ chains we tested. This result shows that enzyme delivery to lysosomes was not impaired—consistent with the existence of multiple transport routes (Gieselmann *et al.*, 1983; Glickman and Kornfeld, 1993; Isidoro *et al.*, 1998; Puertollano *et al.*, 2001; Robinson, 2004). Next we quantified lysosomal enzyme release under each knockdown condition. Much like Lamp1 appearance at the cell surface (Figure 7, D and F), μ3 knockdown using three different target sequences only marginally affected ionomycin-induced secretion of hexosaminidase (Figure 7G, Supplemental Figure S2D) or cathepsin D (Figure 7H), when compared with mock-treated controls. By contrast, and consistent with Lamp1 biotinylation (Figure 7F), both μ1 and μ2 depletion caused a significant reduction in the release of hexosaminidase (Figure 7G and Supplemental Figure S2) and mature cathepsin D (Figure 7H)—but, in contrast to Lamp1, these enzymes did not accumulate on the surface after μ2 depletion, because they are soluble and are not cycling.

The effects of μ1 knockdown are unlikely to be due to some nonspecific or off-target effects of the siRNAs. Indeed, the ionomycin-induced release of both hexosaminidase and cathepsin D as well as Lamp1 appearance on the cell surface were also inhibited by treatment with another siRNA (mu1si#2) against a different μ1 target sequence (Supplemental Figure S2, A–C). Moreover, knockdown of the γ1 subunit of AP1, albeit only partial, also reduced endo-lysosome exocytosis (Supplemental Figure S2E), as did the knockdown of clathrin heavy chain

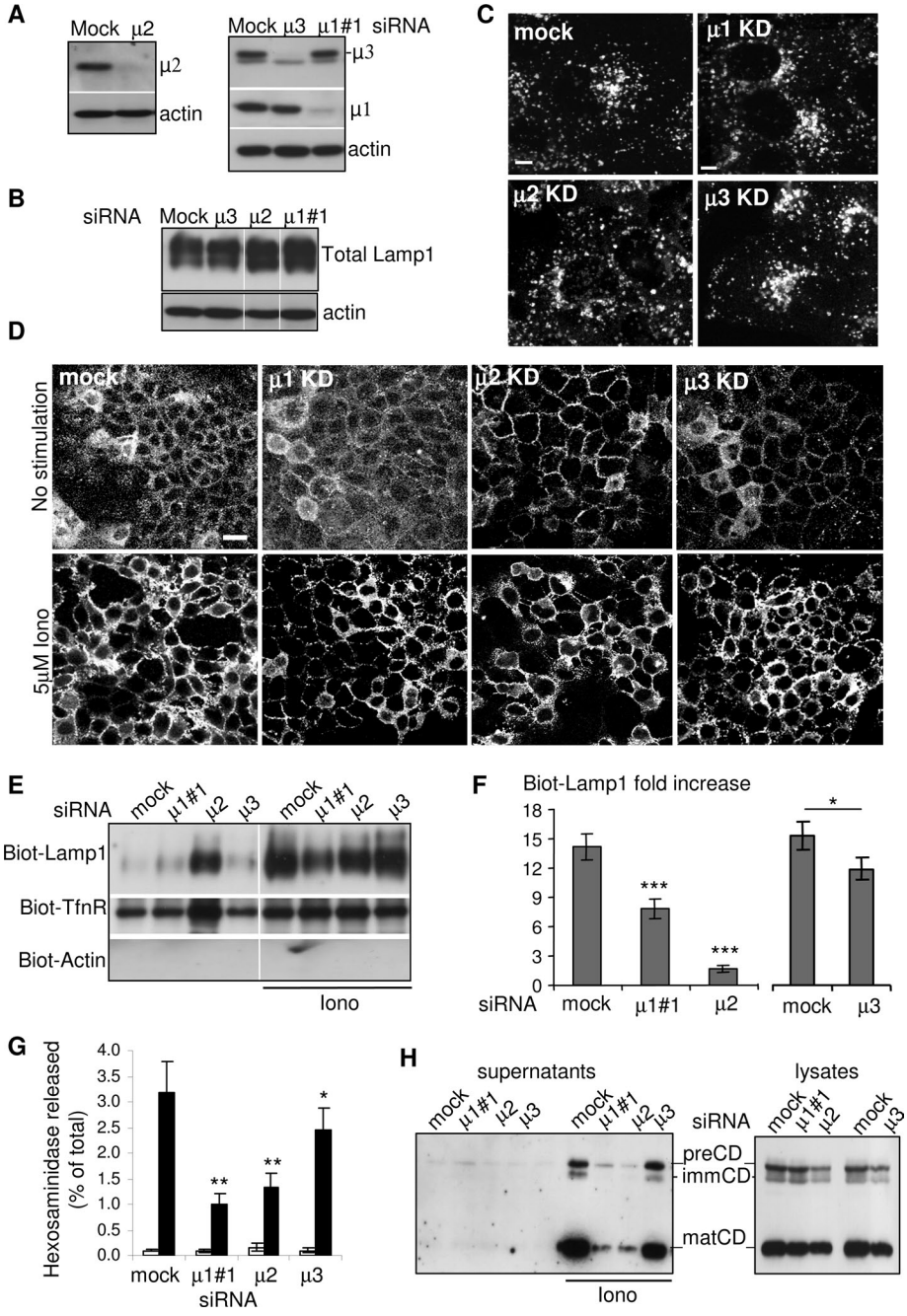

FIGURE 7: Role of adaptor protein complexes in calcium-induced exocytosis of endosecretory compartments A431 cells were transfected with siRNAs against the μ chain of AP1, AP2, or AP3 and the KD efficiency was determined by Western blotting (A). Total amount (B) or intracellular distribution (C) of Lamp1 was analyzed in cells depleted for μ1, μ2, or μ3. No difference was observed as compared with control cells. (D) After KD of the indicated μ subunit and stimulation with ionomycin, Lamp1 on the cell surface was labeled as in Figure 1. The micrographs show large overview fields (Bar = 20 μm) obtained with laser scanning a confocal microscope. (E and F) After KD and stimulation as in (D), Lamp1 appearance on the plasma membrane after cell surface biotinylation was analyzed as in Figure 1, E and F. A representative blot is shown in (E), and the data are quantified in (F). Means ± SEM of eight experiments are shown. *$p < 0.04$, **$p < 0.025$, ***$p < 0.0025$. (G and H) After KD and stimulation, hexosaminidase release (G; means of four experiments ± SEM) was measured as in Figure 1A and cathepsin D release (H) was analyzed as in Figure 7C.

(CHC; Supplemental Figure S3). Altogether, our data demonstrate a crucial function of AP1 and AP2 complexes in the regulation of the calcium-induced exocytosis of endo-lysosomes.

Clathrin and lysosomal exocytosis

Next we investigated whether clathrin itself was also involved in this unconventional secretory process, because clathrin is well known to be associated with both AP1- and AP2-dependent sorting and transport steps. CHC could be efficiently depleted with siRNAs (Supplemental Figure S3A), but cells became more fragile. Thus, to avoid possible toxic effects of the combined knockdown and ionomycin treatments, ionomycin was reduced to 2.5 μM (instead of 5 μM) to induce a transient rise in cytosolic calcium.

After CHC depletion with siRNAs, much like after AP2 depletion, Lamp1 was found to accumulate at the plasma membrane by light microscopy (Supplemental Figure S3D) already in nonstimulated cells—and this accumulation was no longer sensitive to ionomycin treatment. This finding is in good agreement with the role of clathrin-mediated endocytosis in Lamp1 cycling (Janvier and Bonifacino, 2005). Similarly, cell surface biotinylation showed that Lamp1—and the Tfn-R, which is also internalized by the clathrin pathway—accumulated at the surface of nonstimulated cells after CHC knockdown (Supplemental Figure S3E). Despite these higher levels of Lamp1 in resting cells, however, CHC depletion still caused some reduction in the appearance of Lamp1 at the plasma membrane after ionomycin treatment, as quantified by cell surface biotinylation (Supplemental Figure S3E). In addition, CHC depletion caused a reduction in the release of both hexosaminidase (Supplemental Figure S3B) and cathepsin D after ionomycin treatment (Supplemental Figure S3C). CHC depletion under these conditions did not appear to interfere with lysosomal enzyme transport or maturation or with lysosome biogenesis, because the total cellular levels of hexosaminidase and cathepsin D remained unaffected (unpublished data). These data show that CHC depletion recapitulates the effects observed after both AP1 and AP2 depletion—in good agreement with the fact that AP1- and AP2-dependent pathways are clathrin-dependent. We conclude that the recruitment of the clathrin coat is necessary for calcium-induced exocytosis of endo-lysosomes, presumably because clathrin and AP1 play a direct role in the secretory process.

The role of the AP1 effector Gadkin

Our observation that endo-lysosome secretion is not affected by BFA (Figure 5) and depends on AP1 (Figure 7) although AP1 is brefeldin-sensitive (Robinson and Kreis, 1992) led us to investigate the possible role of Gadkin/γ-Bar in the process (Schmidt *et al.*, 2009; Maritzen and Haucke, 2010; Maritzen *et al.*, 2010). Indeed,

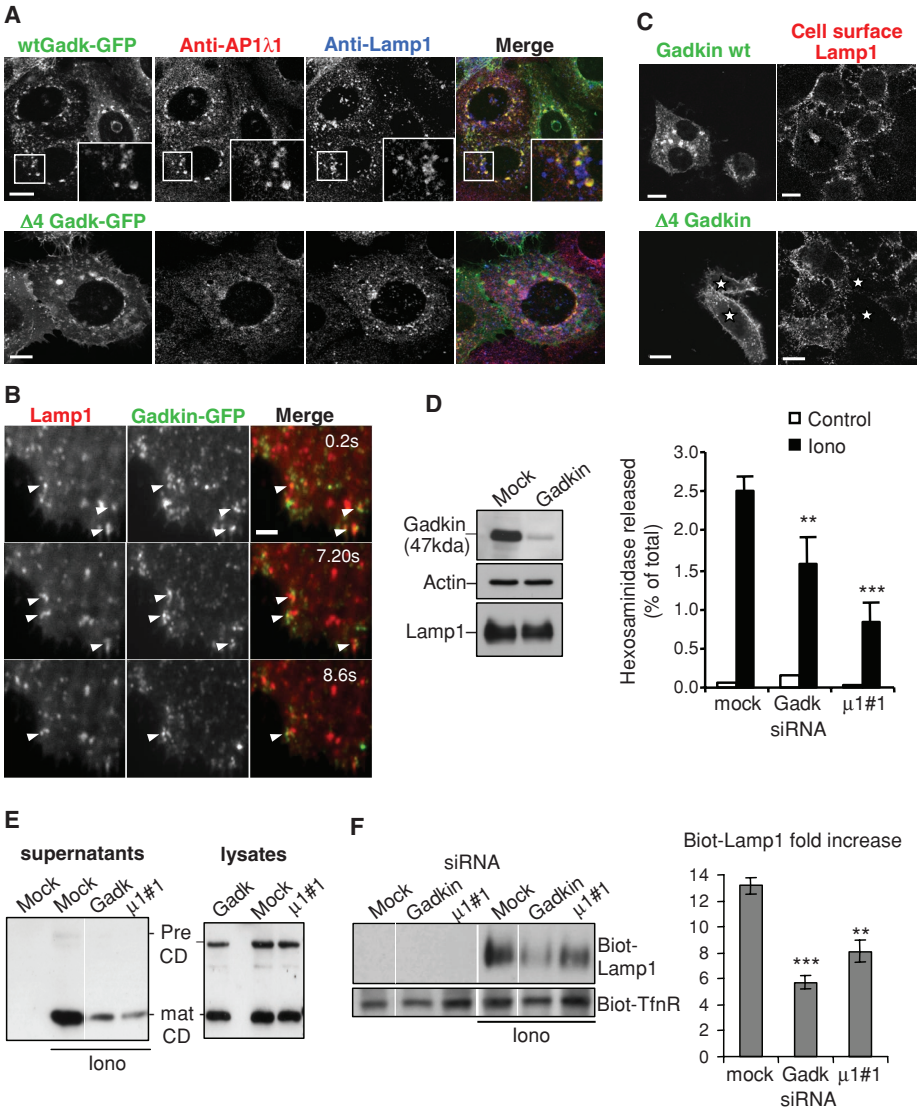

FIGURE 8: Gadkin regulates endo-lysosome exocytosis. (A) Cells transfected with GFP-tagged WT Gadkin (top panel) or Δ4 Gadkin mutant unable to bind AP1γ1 (bottom panel) were fixed, permeabilized, and labeled with anti-AP1γ1 (red) and anti-Lamp1 (blue) antibodies. (B) Cells transfected with WT Gadkin and Lamp1-Cherry were analyzed by time-lapse TIRF microscopy in vivo. Screen captures of Supplementary Movie 6 are shown at the indicated time points. Arrowheads point at structures where Lamp1 and Gadkin are colocalized. Bar = 2.5 µm. (C) Cells transfected as in A were stimulated with ionomycin, and cell surface Lamp1 was labeled as in Figure 1E. Bars = 10 µm (D–F) Cells were transfected with siRNAs against Gadkin (D; KD efficiency ≈ 85–90%) or AP1µ1#1 chain as in A. After ionomycin stimulation, hexosaminidase release (D; means ± SEM of three experiments) was measured as in Figure 1A, cathepsin D release (E) was analyzed as in Figure 5, and Lamp1 appearance on the plasma membrane after cell surface biotinylation (F) was analyzed as in Figure 1, E and F. Means ± SEM of three experiments are shown. **$p < 0.025$, ***$p < 0.0025$.

compartments (Figures 1C and 5, A and B). We thus analyzed the distribution of Gadkin-GFP by time-lapse TIRF microscopy in vivo. Close to the plasma membrane, within the evanescent field of illumination, Gadkin-GFP was found in highly motile vesicles (Figure 8B shows snapshots of Supplemental Movie 6) that were distinct from the perinuclear structures observed by confocal microscopy (Figure 8A). Strikingly, structures containing Gadkin-GFP frequently but often transiently interacted with Lamp1-positive endo-lysosomes (Figure 8B and Supplemental Movie 6). These structures presumably correspond to peripheral Lamp1-positive multivesicular endosomes (Figure 6B)—and Gadkin was found in multivesicular late endosomes (Neubrand *et al.*, 2005).

Next we tested whether Gadkin might be involved in the endo-lysosome secretory process. First, we tested the effects of the Δ4 Gadkin mutant, which no longer binds the γ1 subunit of AP1 (Schmidt *et al.*, 2009). Overexpression of the Δ4 mutant blocked calcium-induced appearance of Lamp1 at the plasma membrane (Figure 8C) without affecting Lamp1 overall distribution (Figure 8B), whereas overexpression of the WT protein had no effect on Lamp1 appearance at the plasma membrane (Figure 8C). Depletion of Gadkin with siRNAs in A431 cells caused a significant decrease in hexosaminidase (Figure 8D) and cathepsin D (Figure 8E) release, without affecting the total cellular levels of either enzyme or the cathepsin D maturation process (unpublished data; Figure 8E)—much like AP1 and clathrin depletion. A similar reduction was observed after knockdown of the γ1 subunit of AP1, although effects were less pronounced, presumably because γ1 depletion was not complete (Supplemental Figure S2E). Finally, we found that Gadkin knockdown (Figure 8F), much like µ1 knockdown (Figure 8F), inhibited the appearance of Lamp1 on the cell surface after ionomycin stimulation. We conclude that Gadkin may act as effector of AP1 in this calcium-induced endo-lysosome secretion, perhaps at the step corresponding to the onset of the secretory event.

Gadkin interacts specifically with the γ1 subunit of AP1 and stabilizes AP1, notably by rendering the adaptor insensitive to BFA (Neubrand *et al.*, 2005).

Gadkin was found to distribute to post-Golgi membranes, the TGN, as well as early and late endosomes and, as expected (Schmidt *et al.*, 2009), showed extensive colocalization in the perinuclear region with the γ1 subunit of AP1 (Figure 8A). Little colocalization between Gadkin and Lamp1 was observed in fixed cells (Figure 8A), in agreement with the fact that Gadkin shows a rather broad distribution and that endo-lysosomes involved in calcium-induced exocytosis represent a small, peripheral subpopulation of all Lamp1-positive

DISCUSSION

Secretory subcompartment(s) of the endocytic pathway

Here we report that a transient rise in cytosolic calcium causes the appearance of Lamp1 at the plasma membrane and the release of lysosomal enzymes in the medium, as observed previously by others (Rodriguez *et al.*, 1997; Andrews, 2000). Not only are the amounts of both Lamp1 and lysosomal enzymes transported to the plasma membrane or secreted small, in the 1% range, but also this process is independent of known endocytic regulators, raising the possibility that the donor membranes used in this unconventional secretory process are not of endocytic but of biosynthetic origin.

Our experiments after inhibition of biosynthetic membrane transport with BFA or ablation of endosomes and lysosomes by HRP-mediated cross-linking, however, unambiguously establish the endocytic nature of the membranes involved in Lamp1 and lysosomal enzyme transport to the plasma membrane. Moreover, our TIRF microscopy analysis in vivo indicates that dynamic Lamp1- and Rab27a-positive vesicles may undergo fusion with the plasma membrane upon ionomycin addition. These observations add further support to the notion that, in nonspecialized fibroblast-like cells, an endocytic compartment acquires secretory properties.

What is then the nature of the endosome or the lysosome population that can dock onto and fuse with the plasma membrane when calcium levels are transiently raised. Selective ablation of sequential endosome populations with endocytosed Tfn-HRP or with a pulse of HRP followed or not by increasing chase time periods indicates that more than one endosome population is sequentially involved in a highly selective and time-defined manner. Our observation that cross-linking early/recycling endosomes inhibits the release of the proform, but not of the mature form, of cathepsin D demonstrates that some early endosome element acquires the capacity to fuse with the plasma membrane—and that late endocytic compartments containing mature enzyme are not affected under these conditions. Conversely, cross-linking late endocytic compartments with HRP selectively inhibits the secretion of mature cathepsin D and active hexosaminidase. By electron microscopy, HRP is found within characteristic multivesicular endosomes containing Lamp1 and Rab27a in the close vicinity of the plasma membrane, after ionomycin treatment. This observation shows that a subpopulation of late endosomes also acquires the specific properties of a secretory organelle after calcium rise.

If both early and late endosome populations can become secretory organelles, one might envision that all late endosomes and lysosomes containing Lamp1 and hydrolases share this property and would be able to fuse with the plasma membrane, provided that cytosolic calcium remains elevated over a longer time course. Several lines of evidence, however, strongly argue against this notion and support the view that this endosecretory process is highly selective. First, a calcium rise certainly did not cause massive fusion of endocytic compartments with the plasma membrane. In fact, cell surface biotinylation of Lamp1 reached a plateau rapidly within 5–10 min and did not increase upon prolonged incubation. Consistently, we could not trigger a second wave of ionomycin-induced hexosaminidase release shortly (5 min) after the first stimulation (unpublished data), strongly suggesting that the fusion-competent pool of membranes had already been exhausted during the first stimulation. In addition, the endosecretory process is fully insensitive to different conditions that inhibit membrane dynamics and motility of late endosomes and lysosomes, including by paralysis at the microtubule-organizing center after Rab7 or RILP overexpression (Jordens *et al.*, 2001; Johansson *et al.*, 2007), cholesterol accumulation (Ko *et al.*, 2001; Lebrand *et al.*, 2002), or depolymerization of microtubules. Hence, this endosecretory process is distinct from lysosome fusion at the ruffled border in osteoclasts, which is sensitive to cholesterol accumulation in late endosomes (Zhao and Vaananen, 2006), although both pathways share with several calcium-dependent exocytic processes a common requirement for synaptotagmin VII (Martinez *et al.*, 2000; Zhao *et al.*, 2008). Moreover, this unconventional secretion pathway depends on actin depolymerization and Rab27a, a small GTPase involved in LRO secretion in specialized cells. This finding agrees well with the role of Rab27a-dependent capture of LROs by F-actin at the cell periphery (Desnos *et al.*, 2003; Barral and Seabra, 2004), reinforcing the notion that

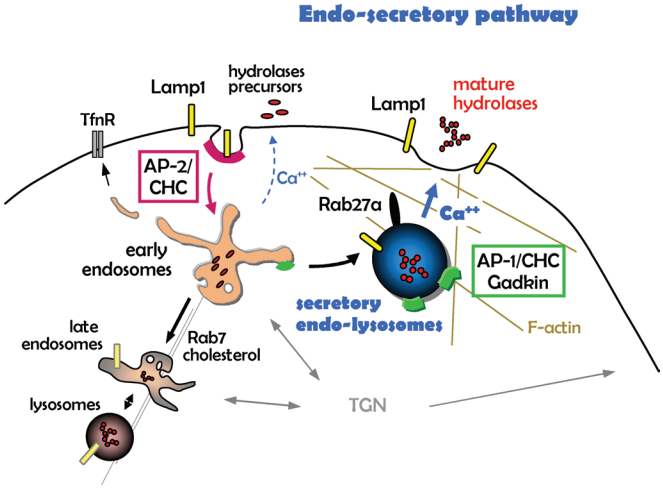

FIGURE 9: Outline of the endosecretory pathway. Endocytic membrane transport from the plasma membrane to early endosomes and then to late endosomes and lysosomes is depicted, as are the proposed roles of AP2, AP1, Gadkin, and Rab27a/actin in endocytosis. We propose that the endosecretory pathway triggered by a transient raise in cytosolic calcium (in blue) bifurcates from the conventional lysosomal pathway at the level of early endosomes.

both processes share common mechanisms. Finally, our in vivo analysis shows that a small subpopulation of vesicles containing Lamp1 and Rab27a, but also Gadkin, show highly dynamic properties in the close vicinity of the plasma membrane, with which they undergo fusion upon transient rise in calcium. These secretory endosomes are also distinct from synaptic microvesicles, because the latter pathway, in contrast to secretory endosomes, is sensitive to BFA and depends on AP3 (Faundez *et al.*, 1997, 1998; Salazar *et al.*, 2004). The simplest interpretation is that the membranes involved in this endosecretory process are distinct from the bulk of endosome and lysosome membranes, and represent specific subpopulations of endocytic membranes along a separate route of membrane traffic, perhaps reminiscent of LRO in specialized cells (model in Figure 9).

Adaptors

We find that the clathrin adaptors AP1 and AP2 regulate this endosecretory process, whereas AP3 does not seem to play a significant role. It has been previously reported that, at steady state, Lamp1 redistributes to the plasma membrane in cells from *mocha* or *pearl* mice in which AP3 δ or ß adaptin is depleted (Dell'Angelica *et al.*, 1999; Reusch *et al.*, 2002; Peden *et al.*, 2004), whereas others (Janvier and Bonifacino, 2005) and we (this study) observed little or no significant change in Lamp1 distribution after μ3 knockdown. This discrepancy may reflect differences caused by the depletion of different AP3 subunits, μ versus δ or ß. Alternatively, they may also be due to long-term consequences of the mutations in the (–/–) mice as opposed to more acute effects of the knockdown. We also find that the secretion of endo-lysosomal subcompartments after a transient rise in calcium is essentially insensitive to μ3 depletion. These observations fit nicely with the findings that AP3 and Rab7 share the same interaction web (Baust *et al.*, 2008) and that NPC1-dependent cholesterol accumulation partially requires AP3 (Berger *et al.*, 2007), but we find that neither Rab7 nor cholesterol are involved in this endosecretory pathway.

We also find that the knockdown of μ2 or CHC increases the steady-state level of Lamp1 at the plasma membrane, supporting the notion that some Lamp1 normally cycles via the plasma

membrane (Lippincott-Schwartz and Fambrough, 1987). The amounts of cell surface Lamp1 remain small (2–3% of total Lamp1) after μ2 knockdown, however, consistent with previous quantification of Lamp1 transport via the plasma membrane (Harter and Mellman, 1992). Unexpectedly, the depletion of μ2 clearly interferes with the secretion of lysosomal enzymes triggered by ionomycin without further increasing Lamp1 levels at the cell surface. This finding might suggest that lysosomal membrane proteins delivered to the plasma membrane after a transient calcium rise belong to a small subpopulation that cycles through the plasma membrane in an AP2- and clathrin-dependent manner.

Finally, our data show that AP1 and clathrin play an essential role in this endosecretory pathway, without affecting the distribution and/or activity of the bulk of lysosomal hydrolases or the distribution of Lamp1. Several recent studies now argue for a direct role of AP1 at the plasma membrane and/or early stages of endocytosis/phagocytosis. The AP1 adaptor may function primarily at the endosome membrane in retrograde transport to the TGN (Meyer *et al.*, 2000; Robinson *et al.*, 2010), and may also be required for correct recycling of synaptic vesicles directly from endosomes (Glyvuk *et al.*, 2010). In addition, evidence indicates that AP1 is also involved in anthrax toxin endocytosis (Abrami *et al.*, 2010), phagocytosis by *Dictyostelium discoideum* (Lefkir *et al.*, 2004), and engulfment of *Listeria monocytogenes* by HeLa cells (Pizarro-Cerda *et al.*, 2007). Future work will be required to establish the precise role of AP1 in unconventional calcium-induced secretion. Some insights into AP1 functions, however, can already be obtained from our findings that the process depends on the AP1 accessory protein Gadkin (Neubrand *et al.*, 2005; Schmidt *et al.*, 2009; Maritzen and Haucke, 2010; Maritzen *et al.*, 2010). The strong effect of μ1, γ1, and Gadkin knockdown shows that other adaptors or accessory factors do not substitute for AP1 or Gadkin in the process, including in particular GGAs that are also involved in clathrin-dependent transport between TGN and endosomes (Bonifacino, 2004), arguing for a highly specific function of AP1 and Gadkin. Our observations that Gadkin, which is required for calcium-induced secretion, is present on highly motile peripheral vesicles, where it colocalizes with Lamp1, through frequent, but often transient interactions, strongly suggest that Gadkin acts on secretory endosomes (see model in Figure 9). It is possible that AP1-clathrin–sorting functions, perhaps orchestrated by Gadkin, regulate this unconventional secretory process. Alternatively, one may speculate that Gadkin regulates secretory endosome–cytoskeleton interactions (model in Figure 9). Indeed, the current view is that LROs in specialized cells are transported to the cell periphery on microtubules and retained by interactions with cortical actin, with Rab27a promoting the microtubule–actin switch (Desnos *et al.*, 2003; Mizuno *et al.*, 2007). Secretory endosomes appear to share with LROs the function of Rab27a and the role of F-actin, presumably reflecting organelle capture at the cell periphery. Interestingly, Gadkin was shown to interact with the microtubule-based motor kinesin (Schmidt *et al.*, 2009), and recent studies suggest that Gadkin is also linked to the actin cytoskeleton (Tanja Maritzen and Volker Haucke, unpublished data). It is thus attractive to propose that AP1 and Gadkin are involved in calcium-induced endosome secretion by controlling the selective interactions with the cytoskeleton at the cell periphery.

MATERIALS AND METHODS

Cell culture

Baby hamster kidney cells (BHK21) were grown as described (Gruenberg *et al.*, 1989). Likewise, A431 (human epithelial carcinoma cell line) cells were grown in DMEM-Glutamax (Life Technologies, Carlsbad, CA), 10% fetal calf serum, and 1% penicillin–streptomycin.

Reagents and antibodies

We obtained mouse monoclonal antibodies against the following antigens: exoplasmic domain of human Lamp1 (H4A3) and CHC from BD PharMingen (San Diego, CA), actin (AC15) from Abcam (Cambridge, UK), Tfn-R from Zymed (San Francisco, CA), μ chain of AP2 from Epitomics (Burlingame, CA), μ chain of AP3 (p47A) from BD PharMingen, γ chain of AP1 (BD PharMingen), tubulin from Sigma-Aldrich (St. Louis, MO), human cathepsin D from Calbiochem (San Diego, CA) and BD PharMingen. We obtained rabbit polyclonal antibodies against the tumor suppressor p53 from Abcam, against Rab6 and goat anti-TGN38 from Santa Cruz Biotechnology (Santa Cruz, CA), and sheep polyclonal antibodies against the epidermal growth factor (EGF) receptor from BD Biosciences (San Diego, CA). The rabbit antibody against the μ chain of AP1 was a gift from P. Schu (Göttingen, Germany). The rabbit polyclonal antibodies against human Gadkin (Maritzen *et al.*, 2010), p23 (Rojo *et al.*, 1997), and GFP (Puri, 2009) were described, as were the monoclonal antibodies against hamster Lamp1 (4A1) (Aniento *et al.*, 1993) and LBPA (6C4) (Kobayashi *et al.*, 1998). The polyclonal anti-HRP antibody was from Sigma-Aldrich. HRP-labeled secondary antibodies were from Amersham Biosciences (GE Healthcare) and Sigma-Aldrich, and fluorescently labeled secondary antibodies and HRP-conjugated Tfn were from Jackson Immunoresearch Laboratories (Suffolk, UK). Transfection reagents were from Invitrogen (Carlsbad, CA). Sulfo-NHS-SS-Biotin (#21331), and streptavidin-beads were from Pierce (Thermo Fisher Scientific, Rockford, IL). Alexafluor 488 Phalloïdin was from Invitrogen. All other chemicals were from Sigma-Aldrich.

DNA, siRNA, and transfections

The following plasmids were gifts: WT-Rab7, Rab7-N125I, and Lamp1 in pEGFP-N1 from P. Boquet (Nice, France); C33-RILP in pEGFP-N1, WT-RILP in pEGFP-C1 from C. Bucci (Lecce, Italy); Lamp1-cherry from J. Lippincott-Schwartz (National Institutes of Health [NIH], Bethesda, MD); Rab27a-GFP from M. Seabra (Imperial College, London, UK). Cells grown on glass slides in six-well dishes were transfected with 1 μg each DNA mixed according to the manufacturer's recommendations with 20 μl Lipofectamine 2000 in 500 μl of OptiMEM and then incubated for ~20 h.

In RNAi experiments, siRNAs against the subunits of AP1, AP2, or AP3, against VSVG used as a control, were obtained from Qiagen (Germantown, MD). The target sequences were: 5′ AAG GCA TCA AGT ATC GGA AGA 3′ (μ1#1), 5′ CCC GAT CAG TGT CAA GTT CGA 3′ (μ1#2), 5′ TGC CAT CGT GTG GAA GAT CAA 3′ (μ2), 5′ AAG GAT AGC CCT TAC ACT CAT 3′ (μ3, siRNA "1"), 5′ ATA GAC GCA ATT ATA GAT AAA 3′ (μ3, siRNA "2"), 5′ CAG GAC TAC TTT GGT GAG TGT 3′ (μ3, siRNA "3"), 5′ GAA GAT AGA ATT CAC CTT TGA 3′ (γ1), 5′ AAA AAG GAA ACT GGA AAA ATG 3′ (VSVG or "mock"), and 5′-AAG ATA GAT GTT CAT ATT GAA-3′ (Rab27a). Against CHC, we used a siRNA pool from Dharmacon targeting the following four sequences: 5′-GAGAATGGCTGTACGTAAT-3′, 5′-TGAGAAATGTAATGCGAAT-3′, 5′-GCAGAAGAATCAACGTTAT-3′, 5′-CGTAAGAAGGCTCGAGAGT-3′; the control siRNA was "ON-TARGET" from Dharmacon. The siRNA against human Gadkin was described (Schmidt *et al.*, 2009): 5′ CGA AGT AGA CTC TCA TCA GAT GCT 3′. Cells were grown in six-well plates for 1 d before siRNA transfection. Then medium was replaced with antibiotic-free medium, and 120 pmol of each siRNA (from 20 μM solutions) were mixed according to the manufacturer's recommendations with 6 μl Lipofectamine RNAiMAX in 1 ml OptiMEM, incubated for 20 min at room

temperature, distributed into two wells, and finally further incubated for 72 h.

Stimulation with calcium ionophores

BHK or A431 cells grown in six-well dishes were washed with phosphate-buffered saline (PBS) at 4°C, and then incubated with 1 ml per well of iso-osmotic HEPES-buffered saline medium (HBS; 120 mM NaCl, 5 mM KCl, 12 mM HEPES, 10 mM D-glucose, 2 mM $CaCl_2$, 2 mM $MgCl_2$) with or without 5 μM ionomycin for the indicated time at 37°C. Kinetics experiments showed that ionomycin treatment becomes toxic after 10 min, and thus all experiments were carried out for a maximum of 10 min, as indicated. When indicated, 1 mM EGTA was added to determine calcium requirements. Then cells were rapidly transferred to an ice bath, and supernatants were collected. Before analysis, cell debris were always removed from supernatants by centrifugation at 4°C for 10 min at 13,000 × *g*. Cells were washed with ice-cold PBS and used in subsequent experiments or lysed in lysis buffer consisting of 20 mM, Tris pH 7.4, 150 mM NaCl, 1 mM EDTA (TNE buffer), supplemented with 10 μg/μl leupeptin, 5 μg/μl aprotinin, 1 μM pepstatin, 10% glycerol, and 1% NP40, using 500 μl per well for 45 min on a rocking platform on ice. Lysates were also clarified before analysis by centrifugation at 4°C for 10 min at 13,000 × *g*.

Quantification of LDH and β-hexosaminidase

Hexosaminidase activity was measured in 96-well plates as described (Andrews, 2000). Briefly, 50 or 100 μl of culture supernatant and 5–10 μl of lysine were mixed with 16 μl of reaction mixture (1 mM 4-methyl-umbellyferyl-*N*-acetyl-β-D-glucosaminide in 11.2 mM citrate/17.6 mM Na_2HPO_4, pH 4.5) completed with PBS to 116 μl. After 30 min at 37°C, the reaction was stopped and amplified by adding 100 μl/well of 2M Na_2CO_3, 1.1 M glycine, pH 10.2, and the fluorescence was measured in a spectrofluorimeter (Gemini XS; Molecular Devices, Sunnyvale, CA), λexc = 365 nm/λem = 450 nm. For LDH measurement, 100 μl of culture supernatant or 10 μl of lysate was mixed with 100 μl of the reaction mixture from the LDH cytotoxicity assay kit (Sigma). After a 20-min reaction at room temperature, the optical density (OD) was measured in a spectrophotometer at 490 nm.

Plasma membrane biotinylation

The plasma membrane of cells grown in six-well dishes was biotinylated for 30 min on ice with 0.5 mg/ml sulfo-NHS-SS-Biotin in PBS containing 1 mM Ca^{++} and 1 mM Mg^{++} (PBS^{++}) (Parton *et al.*, 1992). Then cells were washed with PBS, and the reaction was quenched with 50 mM NH_4Cl in PBS^{++} for 15 min on ice. Finally, cells were washed, lysed in lysis buffer for 45 min, and scraped off the dish with a rubber policeman. After centrifugation at 4°C for 10 min at 13,000 × *g*, equal protein amounts from each lysate were added onto 50-μl streptavidin–bead slurry, and the mixture was incubated overnight at 4°C with constant mixing. Then beads were sedimented at 300 × *g* for 5 min at 4°C and resuspended in diluted lysis buffer (TNE + 0.1% NP40) for washing, repeated three times. Biotinylated proteins were eluted from beads at 95°C for 15 min in gel electrophoresis sample buffer, with regular shaking, as described (Gottardi *et al.*, 1995). When total biotinylated protein quantification was needed, sample buffer without bromophenol blue was used to elute proteins from streptavidin beads upon boiling. Quantification was done with the bicinchoninic acid assay, according to the manufacturer's instruction (BCA assay, Sigma). Biotinylated proteins were analyzed in 9% acrylamide SDS gels. For quantitation, the "plot profile" tool of ImageJ software was used. The "fold increase" corresponds to the ratio between the gray value signals of ionomycin-stimulated over nonstimulated conditions.

Immunofluorescence protocols and plasma membrane Lamp1 labeling

To detect Lamp1 on the plasma membrane, nonpermeabilized cells were washed with chilled PBS immediately after ionomycin stimulation, incubated with anti-Lamp1 antibodies in PBS–5% bovine serum albumin (BSA) on ice for 30 min (Andrews, 2000), fixed for 20 min with PBS–4% paraformaldehyde (PFA), incubated with fluorescent secondary antibodies on ice, and processed for immunofluorescence analysis. When cholesterol was visualized, cells that had been processed as above were treated with 50 μg/ml filipin, which labels cholesterol and can be revealed by UV light (Kobayashi *et al.*, 1999). Slides were observed on a 63× NA 1.4 objective of a Zeiss LSM510 confocal microscope (Thornwood, NY), and pinhole diameters allowed a 0.8-μm optical slice thickness. For TIRF microscopy, samples were imaged at room temperature in HBS without or with 2.5 mM ionomycin, as indicated, using a Zeiss AxioObserver microscope equipped with Zeiss TIRF slider module and HQ2 Camera from Photometrics (Tucson, AZ). Exposure time was 200 ms per frame.

Inactivation of endocytic compartments by HRP-DAB cross-linking in vivo

To inactivate endocytic compartments in vivo, we used the HRP-DAB cross-linking protocol established by Stoorvogel and collaborators (Stoorvogel, 1998). Recycling endosomes can be inactivated after incubation with 20 μg/ml Tfn-HRP in DMEM buffered with 12 mM HEPES, pH 7.4, at 37°C for 20 min. Then cells were washed with ice-cold PBS–5% BSA and incubated on ice with PBS containing 100 μg/ml DAB and 0.003% H_2O_2. Cells were extensively washed with PBS at room temperature and used in further experiments as indicated. To inactivate early endosomes, late endosomes, or lysosomes compartments, the cross-linking protocol was the same, except that cells were pulsed with 0.5 or 5 g/l HRP for 15 min at 37°C, then washed extensively with PBS–5% BSA, followed or not by a 30- or 90-min chase period in HRP-free DMEM.

Other methods

Treatment with 3 μg/ml U18666A for 16 h was described (Kobayashi *et al.*, 1999). Nocodazole, BFA, and latrunculin B were added at the indicated concentration directly to the growth medium for the indicated time periods before washes and stimulation. None of the drugs was present during stimulation with ionomycin. BHK cells were incubated for 24 h at 37°C with 50 μg/ml anti-LBPA (6C4) antibody to label late endosomes with endocytosed antibody (Kobayashi *et al.*, 1998). To detect cathepsin D in culture supernatants, proteins were precipitated using 0.02% deoxycholate and 6% trichloroacetic acid (TCA) (Bensadoun and Weinstein, 1976). Electron microscopy after plastic embedding for HRP analysis (Parton *et al.*, 1992) or after immunogold labeling of cryosections (Griffiths *et al.*, 1984) has been described.

SUPPLEMENTAL MATERIALS

Movies 1–6, Supplemental Figures S1–S3, and corresponding legends are included as supplemental materials.

ACKNOWLEDGMENTS

We are grateful to Brigitte Bernadet, Marie-Claire Velluz, and Charles Ferguson for technical assistance; to Véronique Pons for help with electron microscopy; to Sylvain Loubéry and Marcos Gonzales-Gaitan for help with TIRF; and to Cameron Scott for critically reading

the manuscript. Support to J.G. was from the Swiss National Science Foundation, PRISM from the EU Sixth Framework Programme, LipidX from the Swiss SystemsX.ch initiative evaluated by the Swiss National Science Foundation, and the National Center of Competence in Research (NCCR) in Chemical Biology. Support to T.M. and V.H. was from the German Funding Agency DFG (HA2686/1-3, SFB765/ B4). Support to R.G.P. was from the Human Frontier Science Program Organization.

REFERENCES

Abrami L, Bischofberger M, Kunz B, Groux R, Van Der Goot FG (2010). Endocytosis of the anthrax toxin is mediated by clathrin, actin and unconventional adaptors. PLoS Pathog 6, e1000792.

Andrews NW (2000). Regulated secretion of conventional lysosomes. Trends Cell Biol 10, 316–321.

Andrews NW (2002). Lysosomes and the plasma membrane: trypanosomes reveal a secret relationship. J Cell Biol 158, 389–394.

Aniento F, Emans N, Griffiths G, Gruenberg J (1993). Cytoplasmic dynein-dependent vesicular transport from early to late endosomes. J Cell Biol 123, 1373–1387.

Barral DC, Seabra MC (2004). The melanosome as a model to study organelle motility in mammals. Pigment Cell Res 17, 111–118.

Baust T, Anitei M, Czupalla C, Parshyna I, Bourel L, Thiele C, Krause E, Hoflack B (2008). Protein networks supporting AP-3 function in targeting lysosomal membrane proteins. Mol Biol Cell 19, 1942–1951.

Bensadoun A, Weinstein D (1976). Assay of proteins in the presence of interfering materials. Anal Biochem 70, 241–250.

Berger AC, Salazar G, Styers ML, Newell-Litwa KA, Werner E, Maue RA, Corbett AH, Faundez V (2007). The subcellular localization of the Niemann-Pick Type C proteins depends on the adaptor complex AP-3. J Cell Sci 120, 3640–3652.

Bonifacino JS (2004). The GGA proteins: adaptors on the move. Nat Rev Mol Cell Biol 5, 23–32.

Bonifacino JS, Traub LM (2003). Signals for sorting of transmembrane proteins to endosomes and lysosomes. Annu Rev Biochem 72, 395–447.

Brachet V, Pehau-Arnaudet G, Desaymard C, Raposo G, Amigorena S (1999). Early endosomes are required for major histocompatiblity complex class II transport to peptide-loading compartments. Mol Biol Cell 10, 2891–2904.

Bucci C, Thomsen P, Nicoziani P, McCarthy J, van Deurs B (2000). Rab7: a key to lysosome biogenesis. Mol Biol Cell 11, 467–480.

Cantalupo G, Alifano P, Roberti V, Bruni CB, Bucci C (2001). Rab-interacting lysosomal protein (RILP): the Rab7 effector required for transport to lysosomes. EMBO J 20, 683–693.

Chapuy B, Tikkanen R, Muhlhausen C, Wenzel D, von Figura K, Honing S (2008). AP-1 and AP-3 mediate sorting of melanosomal and lysosomal membrane proteins into distinct post-Golgi trafficking pathways. Traffic 9, 1157–1172.

Clark R, Griffiths GM (2003). Lytic granules, secretory lysosomes and disease. Curr Opin Immunol 15, 516–521.

Czibener C, Sherer NM, Becker SM, Pypaert M, Hui E, Chapman ER, Mothes W, Andrews NW (2006). Ca2+ and synaptotagmin VII-dependent delivery of lysosomal membrane to nascent phagosomes. J Cell Biol 174, 997–1007.

Delevoye C *et al*. (2009). AP-1 and KIF13A coordinate endosomal sorting and positioning during melanosome biogenesis. J Cell Biol 187, 247–264.

Dell'Angelica EC, Shotelersuk V, Aguilar RC, Gahl WA, Bonifacino JS (1999). Altered trafficking of lysosomal proteins in Hermansky-Pudlak syndrome due to mutations in the beta 3A subunit of the AP-3 adaptor. Mol Cell 3, 11–21.

Denzer K, Kleijmeer MJ, Heijnen HF, Stoorvogel W, Geuze HJ (2000). Exosome: from internal vesicle of the multivesicular body to intercellular signaling device. J Cell Sci 113, Pt 19, 3365–3374.

Desnos C *et al*. (2003). Rab27A and its effector MyRIP link secretory granules to F-actin and control their motion towards release sites. J Cell Biol 163, 559–570.

Eder C (2009). Mechanisms of interleukin-1beta release. Immunobiology 214, 543–553.

Faundez V, Horng JT, Kelly RB (1997). ADP ribosylation factor 1 is required for synaptic vesicle budding in PC12 cells. J Cell Biol 138, 505–515.

Faundez V, Horng JT, Kelly RB (1998). A function for the AP3 coat complex in synaptic vesicle formation from endosomes. Cell 93, 423–432.

Fukuda M (2005). Versatile role of Rab27 in membrane trafficking: focus on the Rab27 effector families. J Biochem 137, 9–16.

Gibbings DJ, Ciaudo C, Erhardt M, Voinnet O (2009). Multivesicular bodies associate with components of miRNA effector complexes and modulate miRNA activity. Nat Cell Biol 11, 1143–1149.

Gieselmann V, Pohlmann R, Hasilik A, Von Figura K (1983). Biosynthesis and transport of cathepsin D in cultured human fibroblasts. J Cell Biol 97, 1–5.

Glickman JN, Kornfeld S (1993). Mannose 6-phosphate-independent targeting of lysosomal enzymes in I-cell disease B lymphoblasts. J Cell Biol 123, 99–108.

Glyvuk N, Tsytsyura Y, Geumann C, D'Hooge R, Huve J, Kratzke M, Baltes J, Boening D, Klingauf J, Schu P (2010). AP-1/sigma1B-adaptin mediates endosomal synaptic vesicle recycling, learning and memory. EMBO J 29, 1318–1330.

Gottardi CJ, Dunbar LA, Caplan MJ (1995). Biotinylation and assessment of membrane polarity: caveats and methodological concerns. Am J Physiol 268, F285–F295.

Griffiths G, McDowall A, Back R, Dubochet J (1984). On the preparation of cryosections for immunocytochemistry. J Ultrastruct Res 89, 65–78.

Groux-Degroote S, van Dijk SM, Wolthoorn J, Neumann S, Theos AC, De Maziere AM, Klumperman J, van Meer G, Sprong H (2008). Glycolipid-dependent sorting of melanosomal from lysosomal membrane proteins by lumenal determinants. Traffic 9, 951–963.

Gruenberg J (2001). The endocytic pathway: a mosaic of domains. Nat Rev Mol Cell Biol 2, 721–730.

Gruenberg J, Griffiths G, Howell KE (1989). Characterization of the early endosome and putative endocytic carrier vesicles in vivo and with an assay of vesicle fusion in vitro. J Cell Biol 108, 1301–1316.

Harter C, Mellman I (1992). Transport of the lysosomal membrane glycoprotein lgp120 (lgp-A) to lysosomes does not require appearance on the plasma membrane. J Cell Biol 117, 311–325.

Ihrke G, Kyttala A, Russell MR, Rous BA, Luzio JP (2004). Differential use of two AP-3-mediated pathways by lysosomal membrane proteins. Traffic 5, 946–962.

Isidoro C, Baccino FM, Hasilik A (1998). Human and hamster procathepsin D, although equally tagged with mannose-6-phosphate, are differentially targeted to lysosomes in transfected BHK cells. Cell Tissue Res 292, 303–310.

Jaiswal JK, Andrews NW, Simon SM (2002). Membrane proximal lysosomes are the major vesicles responsible for calcium-dependent exocytosis in nonsecretory cells. J Cell Biol 159, 625–635.

Janvier K, Bonifacino JS (2005). Role of the endocytic machinery in the sorting of lysosome-associated membrane proteins. Mol Biol Cell 16, 4231–4242.

Johansson M, Rocha N, Zwart W, Jordens I, Janssen L, Kuijl C, Olkkonen VM, Neefjes J (2007). Activation of endosomal dynein motors by stepwise assembly of Rab7-RILP-p150Glued, ORP1L, and the receptor betalll spectrin. J Cell Biol 176, 459–471.

Jordens I, Fernandez-Borja M, Marsman M, Dusseljee S, Janssen L, Calafat J, Janssen H, Wubbolts R, Neefjes J (2001). The Rab7 effector protein RILP controls lysosomal transport by inducing the recruitment of dynein-dynactin motors. Curr Biol 11, 1680–1685.

Klausner RD, Donaldson JG, Lippincott-Schwartz J (1992). Brefeldin A: insights into the control of membrane traffic and organelle structure. J Cell Biol 116, 1071–1080.

Ko DC, Gordon MD, Jin JY, Scott MP (2001). Dynamic movements of organelles containing Niemann-Pick C1 protein: NPC1 involvement in late endocytic events. Mol Biol Cell 12, 601–614.

Kobayashi T, Beuchat MH, Lindsay M, Frias S, Palmiter RD, Sakuraba H, Parton RG, Gruenberg J (1999). Late endosomal membranes rich in lysobisphosphatidic acid regulate cholesterol transport. Nat Cell Biol 1, 113–118.

Kobayashi T, Stang E, Fang KS, de Moerloose P, Parton RG, Gruenberg J (1998). A lipid associated with the antiphospholipid syndrome regulates endosome structure and function. Nature 392, 193–197.

Kobayashi T, Vischer UM, Rosnoblet C, Lebrand C, Lindsay M, Parton RG, Kruithof EK, Gruenberg J (2000). The tetraspanin CD63/lamp3 cycles between endocytic and secretory compartments in human endothelial cells. Mol Biol Cell 11, 1829–1843.

Kroemer G, Jaattela M (2005). Lysosomes and autophagy in cell death control. Nat Rev Cancer 5, 886–897.

Le Borgne R, Alconada A, Bauer U, Hoflack B (1998). The mammalian AP-3 adaptor-like complex mediates the intracellular transport of lysosomal membrane glycoproteins. J Biol Chem 273, 29451–29461.

Lebrand C, Corti M, Goodson H, Cosson P, Cavalli V, Mayran N, Faure J, Gruenberg J (2002). Late endosome motility depends on lipids via the small GTPase Rab7. EMBO J 21, 1289–1300.
Lee YS *et al*. (2009). Silencing by small RNAs is linked to endosomal trafficking. Nat Cell Biol 11, 1150–1156.
Lefkir Y, Malbouyres M, Gotthardt D, Ozinsky A, Cornillon S, Bruckert F, Aderem AA, Soldati T, Cosson P, Letourneur F (2004). Involvement of the AP-1 adaptor complex in early steps of phagocytosis and macropinocytosis. Mol Biol Cell 15, 861–869.
Lippincott-Schwartz J, Fambrough DM (1987). Cycling of the integral membrane glycoprotein, LEP100, between plasma membrane and lysosomes: kinetic and morphological analysis. Cell 49, 669–677.
Liscum L, Ruggiero RM, Faust JR (1989). The intracellular transport of low density lipoprotein-derived cholesterol is defective in Niemann-Pick type C fibroblasts. J Cell Biol 108, 1625–1636.
Ludwig T, Griffiths G, Hoflack B (1991). Distribution of newly synthesized lysosomal enzymes in the endocytic pathway of normal rat kidney cells. J Cell Biol 115, 1561–1572.
Ludwig T, Munier-Lehmann H, Bauer U, Hollinshead M, Ovitt C, Lobel P, Hoflack B (1994). Differential sorting of lysosomal enzymes in mannose 6-phosphate receptor-deficient fibroblasts. EMBO J 13, 3430–3437.
Luzio JP, Pryor PR, Bright NA (2007). Lysosomes: fusion and function. Nat Rev Mol Cell Biol 8, 622–632.
Maritzen T, Haucke V (2010). Gadkin: A novel link between endosomal vesicles and microtubule tracks. Commun Integr Biol 3, 299–302.
Maritzen T, Schmidt MR, Kukhtina V, Higman VA, Strauss H, Volkmer R, Oschkinat H, Dotti CG, Haucke V (2010). A novel subtype of AP-1-binding motif within the palmitoylated trans-Golgi network/endosomal accessory protein Gadkin/gamma-BAR. J Biol Chem 285, 4074–4086.
Martinez I, Chakrabarti S, Hellevik T, Morehead J, Fowler K, Andrews NW (2000). Synaptotagmin VII regulates Ca(2+)-dependent exocytosis of lysosomes in fibroblasts. J Cell Biol 148, 1141–1149.
Mayor S, Pagano RE (2007). Pathways of clathrin-independent endocytosis. Nat Rev Mol Cell Biol 8, 603–612.
Meyer C, Zizioli D, Lausmann S, Eskelinen EL, Hamann J, Saftig P, von Figura K, Schu P (2000). mu1A-adaptin-deficient mice: lethality, loss of AP-1 binding and rerouting of mannose 6-phosphate receptors. EMBO J 19, 2193–2203.
Mizuno K, Tolmachova T, Ushakov DS, Romao M, Abrink M, Ferenczi MA, Raposo G, Seabra MC (2007). Rab27b regulates mast cell granule dynamics and secretion. Traffic 8, 883–892.
Neubrand VE, Will RD, Mobius W, Poustka A, Wiemann S, Schu P, Dotti CG, Pepperkok R, Simpson JC (2005). Gamma-BAR, a novel AP-1-interacting protein involved in post-Golgi trafficking. EMBO J 24, 1122–1133.
Novak EK, Gautam R, Reddington M, Collinson LM, Copeland NG, Jenkins NA, McGarry MP, Swank RT (2002). The regulation of platelet-dense granules by Rab27a in the ashen mouse, a model of Hermansky-Pudlak and Griscelli syndromes, is granule-specific and dependent on genetic background. Blood 100, 128–135.
Ostrowski M *et al*. (2010). Rab27a and Rab27b control different steps of the exosome secretion pathway. Nat Cell Biol 12, 19–30; supp 1–13.
Parton RG, Schrotz P, Bucci C, Gruenberg J (1992). Plasticity of early endosomes. J Cell Sci 103, Pt 2335–348.
Peden AA, Oorschot V, Hesser BA, Austin CD, Scheller RH, Klumperman J (2004). Localization of the AP-3 adaptor complex defines a novel endosomal exit site for lysosomal membrane proteins. J Cell Biol 164, 1065–1076.
Pizarro-Cerda J, Payrastre B, Wang YJ, Veiga E, Yin HL, Cossart P (2007). Type II phosphatidylinositol 4-kinases promote Listeria monocytogenes entry into target cells. Cell Microbiol 9, 2381–2390.
Puertollano R, Aguilar RC, Gorshkova I, Crouch RJ, Bonifacino JS (2001). Sorting of mannose 6-phosphate receptors mediated by the GGAs. Science 292, 1712–1716.
Puri C (2009). Loss of myosin VI no insert isoform (NoI) induces a defect in clathrin-mediated endocytosis and leads to caveolar endocytosis of transferrin receptor. J Biol Chem 284, 34998–35014.
Rao SK, Huynh C, Proux-Gillardeaux V, Galli T, Andrews NW (2004). Identification of SNAREs involved in synaptotagmin VII-regulated lysosomal exocytosis. J Biol Chem 279, 20471–20479.
Raposo G, Fevrier B, Stoorvogel W, Marks MS (2002). Lysosome-related organelles: a view from immunity and pigmentation. Cell Struct Funct 27, 443–456.
Raposo G, Marks MS, Cutler DF (2007). Lysosome-related organelles: driving post-Golgi compartments into specialisation. Curr Opin Cell Biol 19, 394–401.
Raposo G, Tenza D, Mecheri S, Peronet R, Bonnerot C, Desaymard C (1997). Accumulation of major histocompatibility complex class II molecules in mast cell secretory granules and their release upon degranulation. Mol Biol Cell 8, 2631–2645.
Reddy A, Caler EV, Andrews NW (2001). Plasma membrane repair is mediated by Ca(2+)-regulated exocytosis of lysosomes. Cell 106, 157–169.
Reusch U, Bernhard O, Koszinowski U, Schu P (2002). AP-1A and AP-3A lysosomal sorting functions. Traffic 3, 752–761.
Robinson MS (2004). Adaptable adaptors for coated vesicles. Trends Cell Biol 14, 167–174.
Robinson MS, Kreis TE (1992). Recruitment of coat proteins onto Golgi membranes in intact and permeabilized cells: effects of brefeldin A and G protein activators. Cell 69, 129–138.
Robinson MS, Sahlender DA, Foster SD (2010). Rapid inactivation of proteins by rapamycin-induced rerouting to mitochondria. Dev Cell 18, 324–331.
Rocha N, Kuijl C, Van Der Kant R, Janssen L, Houben D, Janssen H, Zwart W, Neefjes J (2009). Cholesterol sensor ORP1L contacts the ER protein VAP to control Rab7-RILP-p150 Glued and late endosome positioning. J Cell Biol 185, 1209–1225.
Rodriguez A, Webster P, Ortego J, Andrews NW (1997). Lysosomes behave as Ca2+-regulated exocytic vesicles in fibroblasts and epithelial cells. J Cell Biol 137, 93–104.
Rojo M, Pepperkok R, Emery G, Kellner R, Stang E, Parton RG, Gruenberg J (1997). Involvement of the transmembrane protein p23 in biosynthetic protein transport. J Cell Biol 139, 1119–1135.
Salazar G, Love R, Styers ML, Werner E, Peden A, Rodriguez S, Gearing M, Wainer BH, Faundez V (2004). AP-3-dependent mechanisms control the targeting of a chloride channel (ClC-3) in neuronal and non-neuronal cells. J Biol Chem 279, 25430–25439.
Schmidt MR, Maritzen T, Kukhtina V, Higman VA, Doglio L, Barak NN, Strauss H, Oschkinat H, Dotti CG, Haucke V (2009). Regulation of endosomal membrane traffic by a Gadkin/AP-1/kinesin KIF5 complex. Proc Natl Acad Sci USA 106, 15344–15349.
Stoorvogel W (1998). Analysis of the endocytic system by using horseradish peroxidase. Trends Cell Biol 8, 503–505.
Stoorvogel W, Kleijmeer MJ, Geuze HJ, Raposo G (2002). The biogenesis and functions of exosomes. Traffic 3, 321–330.
Theos AC *et al*. (2005). Functions of adaptor protein (AP)-3 and AP-1 in tyrosinase sorting from endosomes to melanosomes. Mol Biol Cell 16, 5356–5372.
Trajkovic K, Hsu C, Chiantia S, Rajendran L, Wenzel D, Wieland F, Schwille P, Brugger B, Simons M (2008). Ceramide triggers budding of exosome vesicles into multivesicular endosomes. Science 319, 1244–1247.
Zaidi N, Maurer A, Nieke S, Kalbacher H (2008). Cathepsin D: a cellular roadmap. Biochem Biophys Res Commun 376, 5–9.
Zeelenberg IS *et al*. (2008). Targeting tumor antigens to secreted membrane vesicles in vivo induces efficient antitumor immune responses. Cancer Res 68, 1228–1235.
Zerial M, McBride H (2001). Rab proteins as membrane organizers. Nat Rev Mol Cell Biol 2, 107–117.
Zhang M, Dwyer NK, Love DC, Cooney A, Comly M, Neufeld E, Pentchev PG, Blanchette-Mackie EJ, Hanover JA (2001). Cessation of rapid late endosomal tubulovesicular trafficking in Niemann-Pick type C1 disease. Proc Natl Acad Sci USA 98, 4466–4471.
Zhao H, Ito Y, Chappel J, Andrews NW, Teitelbaum SL, Ross FP (2008). Synaptotagmin VII regulates bone remodeling by modulating osteoclast and osteoblast secretion. Dev Cell 14, 914–925.
Zhao H, Vaananen HK (2006). Pharmacological sequestration of intracellular cholesterol in late endosomes disrupts ruffled border formation in osteoclasts. J Bone Miner Res 21, 456–465.